T.C.
ALTINBAŞ UNIVERSITY
Institute of Graduate Studies
Mechanical Engineering

ENHANCEMENT OF AIR COOLING IN TUBE FITTED WITH MULTI-SPRING WIRE AND STUDY FRICTION FACTOR AND EXERGY EFFICIENCY NUMERICALLY

Mahmoud Ali MAHMOUD

Master Thesis

Supervisor

Asst. Prof. Dr. Ibrahim KOC

Istanbul, 2020

ENHANCEMENT OF AIR COOLING IN TUBE FITTED WITH MULTI-SPRING WIRE AND STUDY FRICTION FACTOR AND EXERGY EFFICIENCY NUMERICALLY

by

MAHMOUD, Mahmoud Ali

Mechanical Engineering

Submitted to the Institute of Graduate Studies

in partial fulfillment of the requirements for the degree of

Master of Science

ALTINBAŞ UNIVERSITY

2020

The thesis titled **"ENHANCEMENT OF AIR COOLING IN TUBE FITTED WITH MULTI-SPRING WIRE AND STUDY FRICTION FACTOR AND EXERGY EFFICIENCY"** prepared and presented by **Mahmoud.A. MAHMOUD** was accepted as a Master of Science Thesis in Mechanical Engineering.

Asst. Prof. Dr. İbrahim KOÇ

Supervisor

Thesis Defense Jury Member:

Asst. Prof. Dr. İbrahim KOÇ	School of Engineering and Natural Sciences, Altınbas University	_____
Prof. Dr.Aydın ŞALCI	School of Engineering and Natural Sciences, Altınbas University	_____
Prof.Dr.Cem PARMAKSIZOĞLU	Faculty of Instruments, Mechanical Engineering Department, Istanbul Technical University	_____

I certify that this thesis satisfies all the requirements as a thesis for the degree of Master of Science.

Approval Date of Institute of Graduate studies:

__/__/__

I hereby declare that all information in this document has been obtained and presented in accordance with academic rules and ethical conduct. I also declare that, as required by these rules and conduct, I have fully cited and referenced all material and results that are not original to this work.

Mahmoud.Ali.Mahmoud

DEDICATION

I would like to dedicate this work to my very first teacher, my mother, my first supporter and role model, and my companion throughout the journey and my brothers. Without you, this dream would never come true.

ACKNOWLEDGEMENTS

I might want to offer my thanks to every one of the individuals who have upheld me all through the regularly extended periods of this voyage. I might want to thank my advisor, Asst. Prof. Dr. Ibrahim Koc for being my compass notwithstanding, when I believed I was lost and being in extraordinary part in charge of the zenith of this work. I might likewise want to thank my supervisor for his supportive exhortation, which incredibly enhanced the nature of this work. Finally, I thank this institution for hosting me during these years, securely earning its place as my home. I am very thankful to my mom and dad, whose values and education motivate me to keep asking questions; to my siblings and family for their infinitely appreciated love and to my country which, although inanimate, keeps me anchored and offers me an example of resiliency.

ABSTRACT

ENHANCEMENT OF AIR COOLING IN TUBE FITTED WITH MULTI-SPRING WIRE AND STUDY FRICTION FACTOR AND EXERGY EFFICIENCY NUMERICALLY

Mahmoud, A.Mahmoud

M.S.,Mechanical Engineering Altınbaş University,

Supervisor: Asst. Prof. Ibrahim KOC

Date: August, 2020

Pages: 64

Increasing turbulence and mixing between boundaries in tubes leads to heat transfer enhancement. That can be useful for air cooling in air systems for developing energy efficiency, reduce size and costs. In this thesis, the enhancement of air cooling in a tube fitted with multi-spring wire and study friction factor is introduced and exergy efficiency numerically to increase cooling of air in tubes. The numerical model was validated with a previous experimental study and the results had a high degree of accuracy. The simulation investigation was finished with a range of Reynolds numbers from 2800 to 18000 to refuge the turbulence region. The results showed that the triple spring achieved the highest value of enhancement of air cooling comparing to single and double springs and plain tubes. The triple spring's configuration has the highest heat flux following the figure of 322 to 399 W/m^2. Heat transfer increases easily through the flow and swirls cause flow to be turbulent which led to even better convection heat transfer. Friction factor decrease with the increase of the Reynolds number and the three springs wire has the maximum value. The exergy efficiency increase with the Reynolds number and the higher the number of springs in the tube, the higher the value of the exergy efficiency so that the triple spring has the maximum value of the exergy efficiency comparing to other configurations in this study. It can be observed that the Nusselt number increased with the increase in wire diameter, where the 3 mm wire achieved the

maximum heat transfer enhancement. The four springs with a diameter of 3 mm have a friction factor ranging from 0.1 to 0.2 where the diameter of 1 mm is between 0.05 and 0.15. It can be assumed that the optimal situation was achieved with a 3 mm wire. The increase in diameter from 2 mm to 3 mm results in a 109 percent improvement in exergy efficiency. It can be observed that with the rise of pitch length the Nusselt number improved where the case of 30 mm pitch length reached the extreme enhancement in heat transfer. The increase in the impact of the pressure drop overcomes the rise in the Nusselt number in the case of 30 mm, so that the author selects the second 30 mm configuration as the better alternative. The optimal cold water volumetric flow rate was calculated with three numbers of cold water volumetric flow rates (e.g. 1 LPM, 2 LPM, and 3 LPM). It can be observed that with the increase of Reynolds number as well as the growth of volumetric flow rates of cold water, the Nusselt number enhanced. The optimum condition has 4 springs with a 3 mm wire diameter and 30 mm pitch length where the volumetric flow rate that achieved the optimization was 3 LPM.

Keywords: Air cooling, friction factor, exergy efficiency, multi-springs wire

TABLE OF CONTENTS

Pages

LIST OF TABLES

Pages

LIST OF FIGURES

Pages

LIST OF ABBREVIATIONS

A_S	Surface area, m^2
L	Length of the tube, mm
M_a	Mass flow rate of air, kg/s
M_w	Mass flow rate of water, kg/s
D	Outer diameter, mm
P	Pitch length, mm
T	Temperature, ◦C
C_p	Specific heat, J/kg.K
Q	Heat transfer rate, W
G	Gravity acceleration, m/s^2
Re	Reynolds number
Pr	Prandtl number
U	Overall heat transfer coefficient, W/m^2K
V	Velocity, m/s
H	Heat transfer coefficient, J/kg
K	Thermal conductivity, W/mK
Nu	Nusselt number
LPM	Liter per minute
out	Out
in	In
ave	Average
M_a	Mass flow rate of air
M_w	Mass flow rate of water
Nu	Nusselt number

LIST OF SYMBOLS

ΔP	Pressure drop
η_e	Exergy efficiency
ρ	Density of water
f	Friction factor

1. INTRODUCTION

Nowadays, thermal energy saving is one of the most crucial subjects because of the increase in the utilizing the energy in all fields. Cooling processes to decrease the energy have many up to date developments in many applications. It is important to improve heat transfer and increase efficiency when designing thermal systems. Furthermore, reducing the production costs and developing a smaller thermal device is of great importance for the industry. Air cooling is used in many applications such as refrigeration, air conditioning, food saving, dryness process, and others. Many methods utilized to enhance the air cooling inside tubes like utilizing inserts, fins, and geometry modifications in the wall of the tube.

1.1 THEORY OF AIR COOLING

To decrease the temperature of the air that utilized for process, other fluid with lower temperatures used for cooling such as water, oil, freon. The heat transfers from the fluid that have high temperatures to fluid that have low temperature. Air passes over the low-temperature surface so that the heat moves from air to the surface.

1.2 METHODS OF ENHANCEMENT AIR COOLING

In the past decade, air cooling enhancement has been developed and widely applied to many applications. Augmentative heat transfer aims to accommodate high heat fluxes (or heat transfer coefficient). Up to the present, there has been a great attempt to reduce the sizes and cost of the heat exchanger and energy consumption. The most significant variable in reducing the size and the cost of the heat exchanger, which generally leads to less capital cost and another advantage, is the reduction of the temperature driving force, which increases the second law efficiency and decreases the entropy generation. Thus, this captivates the interests of this thesis. The great attempt on utilizing different methods is to increase the heat transfer rate through the compulsory force convection. There are three methods (i.e. Passive method, active method, and combined passive and active methods) to increase the heat transfer rate. The passive method depends on surface or geometrical modifications without external power such as treated surfaces, twisted tapes, wire helical screw rough surfaces, and extended surfaces, or by use of various inserts. Such inserts include enhancement devices, twisted tape, wire coil, swirl flow generator coiled tubes, surface

tension devices, and additives for gases and liquids. The second method is the active method that uses an external power such as implementing magnetic field reciprocating plungers, the suction of the fluid for flow disturbance, using surface or flow vibration, and applying electromagnetic fields. The third method is the compound method that combines both active and passive methods.

1.3 AIR COOLING APPLICATION

Low-temperature air used in many applications including food saving, refrigeration, air conditioning, dryness process, generator, condenser, radiator, evaporator, and cooling tower. Figure 1.1 shows the air conditioning system with phase change material (PCM) where $T_{a,i}$, $T_{a,E,o}$ express the temperature at the inlet and outlet of the evaporator , respectively. W_{comp} is the work of the compressor, Air cooling used in electronic and information processing equipment requiring rigid climatic conditions for reliable operation with precise temperature control, computer room precision air conditioning, Precision Air Conditioners, and Close Control Unit.

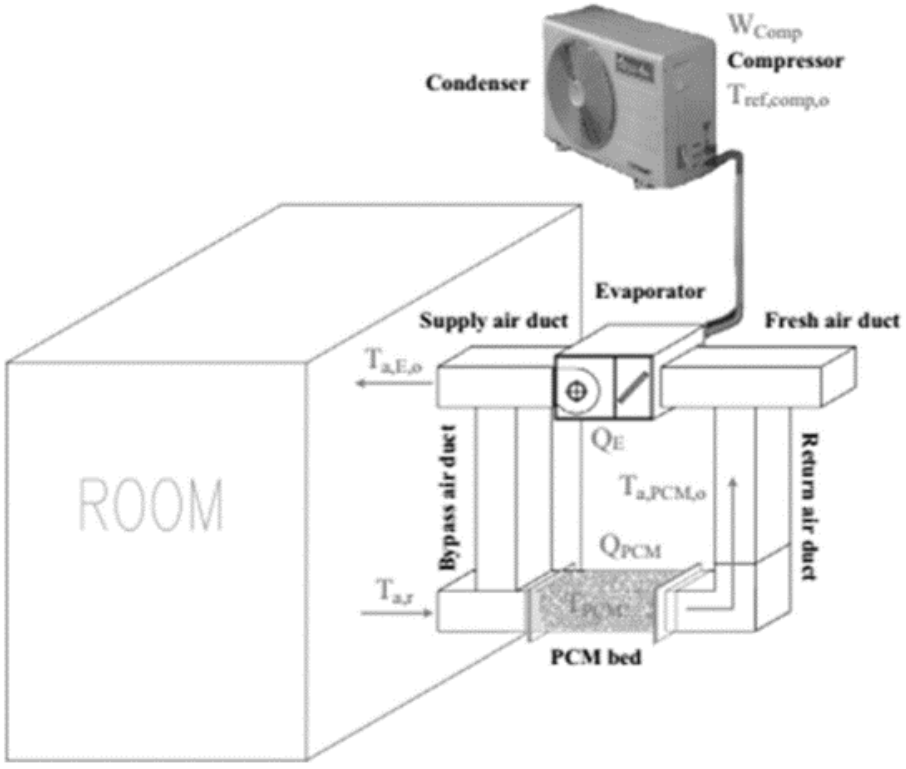

Figure 1.1: Air conditioning system

2. LITERATURE REVIEW

2.1 INTRODUCTION

Nowadays, the reduction of air temperature is fundamental in many applications like air conditioning, air handling unit, and cooling systems. Increasing energy efficiency to decrease size and costs is a vital factor in the design of air cooling systems. Heat transfer and friction factors of the tube are fundamental to study so that the heat coefficient can be increased and pressure losses decreased. Spring wires used to enhancing heat transfer by generating swirl flow which increases the fluid mixing between the boundaries near to the wall and central region.

Al-Fahed and Chakroun [2] studied experimentally the effect of tube-tape clearance on heat transfer in an isothermal tube with a fully turbulent flow. They found that decreasing tube-tape clearance increases the heat transfer improvement. However, at the smaller value of twist ratio, the loose-fit tape offered nearly equivalent heat transfer rate as that provided by the tight-fit twisted tape. Stout et al [3] developed an experimental flood correlation as a function of the tilt angle for a fluted tube with a twisted insert to be used for absorption heat pump systems. Fluted tubes were used during the absorption and desorption processes to facilitate both heat and mass transfer. To contrast current absorption, plastic twisted tape was added to improve the absorption rate with the investigation of the special effects of the twisted insert and inclination angle. Water-ethyl alcohol solution flows downward in the fluted tube while air flows counter current in an upward direction. The findings indicate that flooding was started from the top for angles of inclination less than 60 °, while it began for angles greater than 60 ° from the bottom of the channel. The variations in pressure drop were very high when flooding began from the bottom whereas when it began from the top, it was not as high. The impact of the insert positions for the nearly horizontal tube was not considerable, while it had some influence on the vertical tube. The flood vapor velocity was the maximum for the inclination angle between 40 ° and 60 ° for surface liquid velocities below $1.178\times l0^{-2}$ m / s for the fluted tube with an insert. If the surface velocity of liquid flow is greater than 1.178×10^{-2} m / s, the rate of the surface flooding vapor improves with a change in the angle of inclination.

Takahashi and Momozaki [4] studied the pressure drop and heat transfer of a single-phase mercury flow and a two-phase air – mercury flow in a helical tube under a strong magnetic field. The

pressure drops in a mercury single-phase flow in the absence of a magnetic field agreed with those predicted by the empirical correlations obtained for the pressure drops in a water flow in a helically coiled tube. Pressure drops of a liquid metal in a helically coiled tube could be treated as those in a straight tube, if the Hartmann number is larger than several hundreds, and the interaction parameter is larger than ten, since the centrifugal force is negligibly small compared with the electromagnetic force under the fusion-relevant conditions. Remarkable heat transfer enhancement did not appear by the air injection. Heat transfer was enhanced with increasing the air Reynolds number at high mercury Reynolds number possibly due to the agitation effect of air bubbles. On the other hand, it was deteriorated with increasing the air Reynolds number at low mercury Reynolds number possibly because of the removal of mercury by airflow near the heating wall. Experimentally, Saha *et al.* [5] studied the heat transfer and pressure drop in a tube subjected to a uniform wall heat flux and fitted with twisted tape elements separated by a circular rod. The tape width, rod diameter, and phase angle between consecutive tape elements were varied to observe the variation in the Nusselt number and friction factor. They concluded that reducing the tape widths had a bad effect when comparing with the full width. Besides, increasing the phase angle does not affect thermal-hydraulic performance and increasing the manufacturing complexity. Koyama et al [6] the effect of wire coil insert in vertical round tube on the flow pattern and characteristics in counter-flow. As well as, they studied the void fraction. Aprea and Renno [7] estimated the suitability of the transfer function, the hunting phenomenon, typical of a thermostatic expansion valve experimentally. When the transfer function is applied to this input, the related output is in good agreement with the experimental results. The transfer function of the evaporator system allows the determination of the appropriate values of the refrigerant mass flow rate when the plant working conditions vary. The next step is to identify a control algorithm and implement it on a vapor compression refrigeration plant, while varying the speed of the compressor motor by means of an inverter that acts on the frequency and voltage of the current.

Wang and Sundén [8] investigated correlations for twisted tape and wire coil inserts in both laminar and turbulent regions, and performance comparison is provided. a comprehensive comparison of the thermal and hydraulic performance for these two tube inserts is carried out. Based on empirical correlations a comprehensive comparison of thermal and hydraulic performance for twisted tape and wire coil inserts was performed. Both tube inserts are very effective in heat transfer enhancement, but are more effective in the laminar region than in the turbulent region. As well, the findings show that both tube inserts are more

suitable for high viscosity fluids. If no pressure drop penalty is considered, twisted tape insert is more efficient than a wire coil insert. But wire insert coil gives better overall performance when considering the pressure drop penalty. These results are very useful in applying enhanced heat transfer. Wu et al [9] experimentally investigate the friction characteristics of air flowing through a horizontal circular tube with strip-type inserts. The paper addresses the flow characteristics, which are responsible for the heat transfer enhancement. The average temperature of the airflow protected in this friction study was kept at 26 C^o approximately. The hydrodynamic entry length with a tube insert was found to be shorter than that of a bare tube. The azimuthal velocity profile and turbulent intensity show that symmetry in the angular profile exists for all the cases under study. Mean velocity for the law of the wall was developed for all the cases studied. Friction factor increases for tubes with inserts as compared to bare tube values were typically between 1.1 and 1.5 for where the Reynolds change from 6500 to 19500.

Sharma et al [10] investigated experimentally and numerically the effect of cooling with SiO_2/water nanofluid for a wide range of Reynolds numbers and concentration. The results from the numerical model for different operating conditions are compared with the experimental data and for predicting the flow characteristics. The experimental results indicate a 29.6% enhancement in heat transfer coefficient and 23.7% greater friction factor at 3.0% concentration when compared to water at a twist ratio of 5.0. The values are 94.1% and 160% greater compared to the flow of water in a tube. The heat transfer coefficients decrease when undertaken for concentrations greater than 3.0% at the nanofluid bulk temperature of 30 ºC. Özceyhan [11] simulated the conjugate heat transfer taking place in the wire coil inserted tube. The flow was assumed to be fully developed, and uniform heat was supplied through the external surface of the tube. A numerical technique was used for solving the governing flow, energy, and stress equations. The study also includes the effects of the pitch to diameter ratio of the tube. The temperature and thermal stress distributions of the tube sheet of wire coiled tubes have been presented for different pitches and water inlet velocities to give information for heat transfer exchanger designers. The thermal stresses in the smooth tube have also been analyzed to compare with those in the tube with wire coil inserts. The smooth tube has lower thermal stresses when compared to the wire coil inserted tube for all water velocities. In general, the stress decreases to the minimum at some location on the inner side of the tube sheet. The extreme thermal stresses occur at the outer side of the tube sheet because of

the higher temperature difference magnitude. The stress ratio increases as the volume flow rate of the fluid decreases. The maximum thermal stress ratio occurred in the pitch to diameter ratio equals to 2 and 3 m/s mean water inlet velocity. Tandiroglu [12] studied the effect of flow geometry parameters on transient heat transfer for turbulent flow in a circular tube with baffle inserts The main objective of the present work is to derive empirical equations to correlate the time-averaged friction factor, time-averaged Nusselt number depending on baffle geometry parameters of the pitch to diameter ratio, baffle orientation angle, the ratio of smooth to baffled cross-section area and the ratio of tube length to baffle spacing. The proposed correlations are considered to be applicable within the range of Reynolds number from 3000 to 20,000 for the case of constant heat flux. To this end, the present investigation has been undertaken and it is intended to contribute to the previous and further studies. It may be noticed that the general correlations predict the time-averaged pressure drop data better than the Nusselt number data. Experimental uncertainties in the Reynolds number, friction factor, and Nusselt number were estimated. The mean uncertainties are ±2.5 in the Reynolds number, ±4 in the friction factor. The maximum percentage deviations for the experimental and proposed correlation values of $Nu_{ave(t)}$ and $f_{ave(t)}$ were found to be ±1% for each type of baffle data curve. It can, therefore, be concluded that the proposed correlations are reasonably satisfactory for the prediction of time-averaged Nusselt number and time-averaged pressure drop for baffle inserted tubes.

Heat transfer characteristics and pressure drop of the horizontal double pipes with and without twisted tape insert in the tube side has been studied by Naphon [13] reported that the twisted tape insert has a significant effect on enhancing the heat transfer rate with a drawback of an increase in the pressure drop. Two correlations for the Nusselt number and friction factor were proposed. Variation of the average tube-side heat transfer coefficients with tube-side Reynolds number at the same condition. As expected the average tube-side heat transfer coefficient increases with increasing Reynolds number as the heat transfer coefficient depends directly on the heat transfer rate. Besides, at a given Reynolds number, the average tube-side heat transfer coefficients for tube twisted tape insert are higher than those for plain tubes. Chiu and Jang [14] studied the turbulent three-dimensional fluid gas flow and heat transfer over longitudinal strip inserts and twisted-tape inserts with three different twisted angle numerically. Conjugate heat transfer for convection in the flow field and heat conduction in the tube inserts were also considered. The tests were carried out with an overall counterflow structure in a shell and tube exchanger. The working fluid in the

face of the tube was cold air, while the shell face was the hot dowtherm fluid. To obtain the heat transfer characteristics of the test section from the experimental data, the method effectiveness-number of the transfer unit was used to determine the overall conductance in the analysis. The results showed that the heat transfer coefficient and the pressure drop in the tubes with the longitudinal strip inserts are 7–16% and 100–170% higher than those of plain tubes without inserts, respectively as seen Figure 2.1 The heat transfer coefficient and the pressure drop using longitudinal strip inserts with holes are 13–28% and 140–220% higher than those of plain tubes. The heat transfer coefficient and the pressure drop of the tubes with twisted-tape inserts are 13–61% and 150–370%, respectively, higher than those of plain tubes.

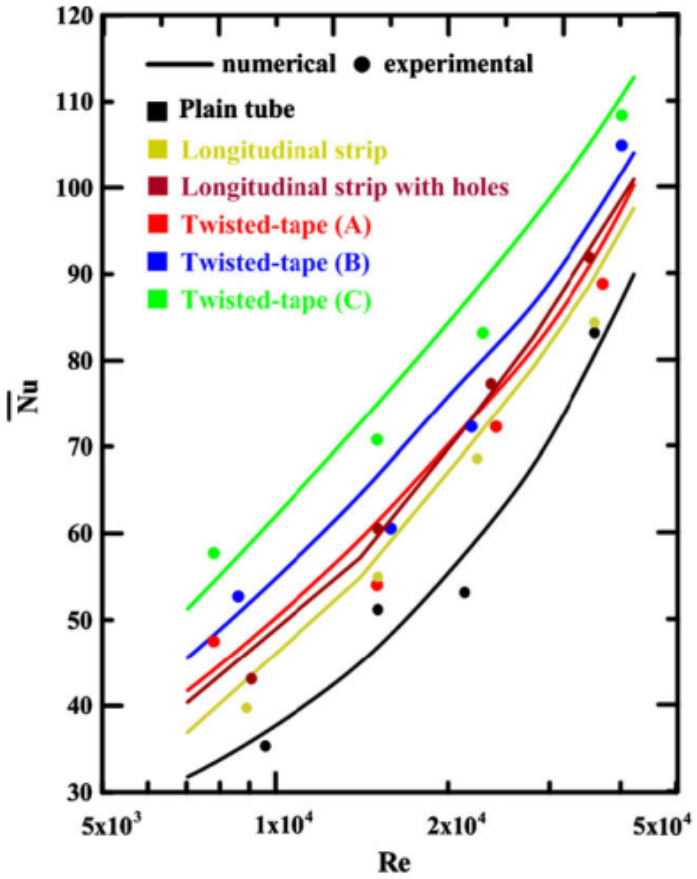

Figure 2.1: The relation between Nusselt number and Reynolds number

Lees et al [15] studied the effect of spiky twisted tape inserts on tubular thermal fluid performance bubbly moving air-water. It can be concluded that with the existence of the spiky twisted-tape insert, the centrifugal forces induce a radial segregating effect that drives the liquid-phase fluid toward the tube wall with the tube core occupied by the gas-phase fluid. Air bubbles in the swirl

tube are drifting within the swirls and concentrated in the core region to enhance collisions and coalescences of bubbles with the radial distribution as the core-peaking profile. While the Nu_S=Nu_P ratios are raised to the similar ranges between the single- and two-phase flows, the presence of two-phase phenomena has neutralized the pressure-drop penalty added by the twisted-tape insert from the total pressure drop across the plain and swirl tubes with air-water flows. As a result, the thermal performance index for each two-phase flow condition is significantly increased from the single-phase level which demonstrates the effectiveness of the present spiky twisted-tape insert for improving the HTE and thermal performances of the tubular air-water bubbly flows. Yadav [16] carried out an experimental study on a U-tube double pipe heat exchanger to study the effect of half-length twisted tape insert in the inner tube side on heat transfer coefficient (h), pressure drop (Δp), and thermal performance factor f_{THP} characteristics compared to the plain heat exchanger. This study concluded that insert improves the heat transfer coefficient by 40%-60%, increases the pressure drop by 0.09 bar-0.27 bar, and reduces the thermal performance factor by 66%-78%. Thianpong et al. [17] predicted experimentally the heat transfer enhancement and pressure loss by use of a dimpled tube with a twisted tape insert. Heat transfer and friction factor were increased with decreasing both of pitch ratio (PR) and twist ratio (y/w). Depending on the pitch ratio and twist ratio, the heat transfer rate and friction factor in the dimpled tube with twisted tape, are respectively 1.66 to 3.03 and 5 to 6.31 times of those in the plain tube. The empirical correlations for the Nusselt number and the friction factor based on experimental data were proposed.

Eiamsa-ard *et al.* [18] performed their experiments to investigate the effect of straight and oblique delta winglet twisted tape (DWT). The experimental work has been carried out with the depth of wing cut ratios of 0.11, 0.21, and 0.31 and twist ratios of 3, 4, and 5. The experimental outcomes showed that the heat transfer coefficient and friction factor rise by reducing the value of twisted ratio and increasing the depth of the wing cut ratio. Nusselt number and friction factor increased with decreasing twist ratio (y/w) and increasing depth of wing cut ratio (DR) for all Reynolds numbers studied as indicated in Figure 2.2. Also, the ordinary DWT gave a higher Nusselt number and friction factor than that of the straight DWT. The thermal performance factor in the tube with oblique DWT was greater than that with straight DWT and it increased with decreasing Reynolds number and increasing twist ratio. Over the range considered, the performance factor in the tubes equipped with the oblique and straight DWTs are found to be around 0.92–1.24 and 0.88–1.21,

respectively. The DWT performed better heat transfer enhancement than that typical twisted tape (TT). It indicated that the heat exchanger fitted with DWT is more compacted than the one with the typical twisted tape. Again, the DWT can be replaced any of the TT efficiently to reduce the size of the heat exchanger.

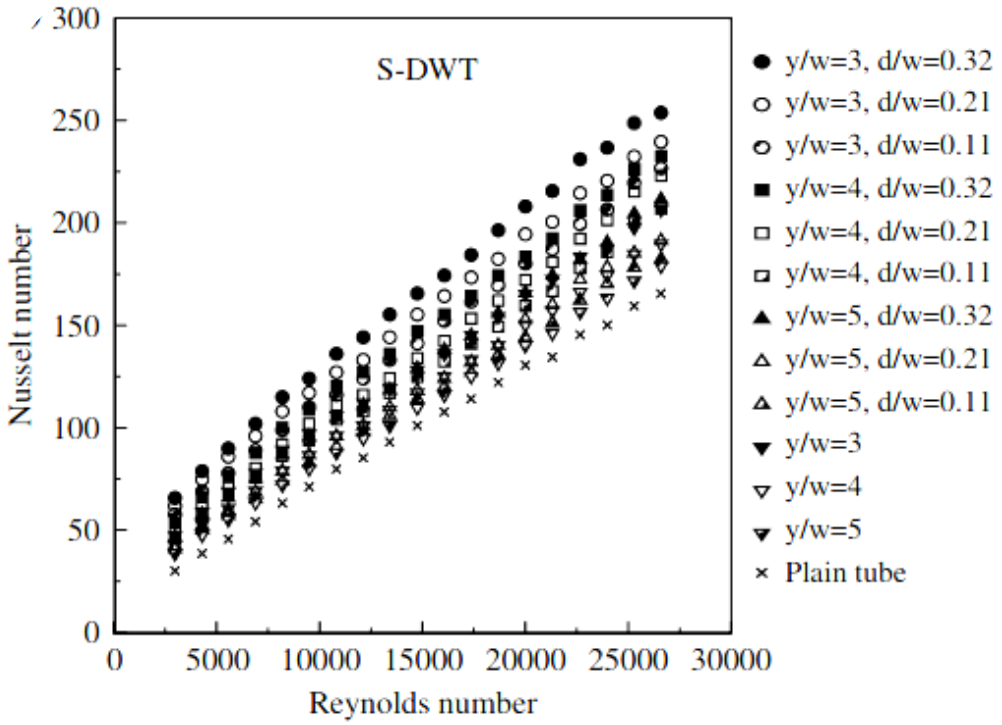

Figure 2.2 Nusselt number versus Reynolds number

Guo et al [19] studied the influence of center twisted tape in the tube on the heat transfer coefficient and pressure drop parameters in case of laminar flow in a circular tube numerically and they finished a comparison between and the short width and the center twisted tapes. It is indicated that both methods lead to a decrease in the pressure resistance. The center-cleared twisted tapes achieved the highest heat transfer rates compared to short-width twisted tapes in the same conditions. Salam et al [20] examined the effect of rectangular cut twisted tape inserted in the tube side on the heat transfer coefficient and pressure drop parameters and compared the results with the plain tubes. The enhancement ratio of heat transfer with the twisted tape (rectangular cut) is 68% comparing to the smooth tube. The friction factor increased by 39% to 80% with inserted tape higher than plain tubes values. Salman et al.[21]finished a numerical study to indicate the effects of quadrant cut twisted tape (QCT) configurations on heat transfer, friction losses, and

swirling flow as well as classical cut twisted tape (CCT). The results showed that the Nusselt number and friction losses increase with quadrant cut twisted tape inserts comparing to the case without inserts for twist ratio (y) and cut depths (w) as seen in Figure 2.3. The reasons for this can be explained as the establishment of vortices troubled the boundaries layers and heat transfer between the fluid at the core and the hot surfaces enhances mixing.

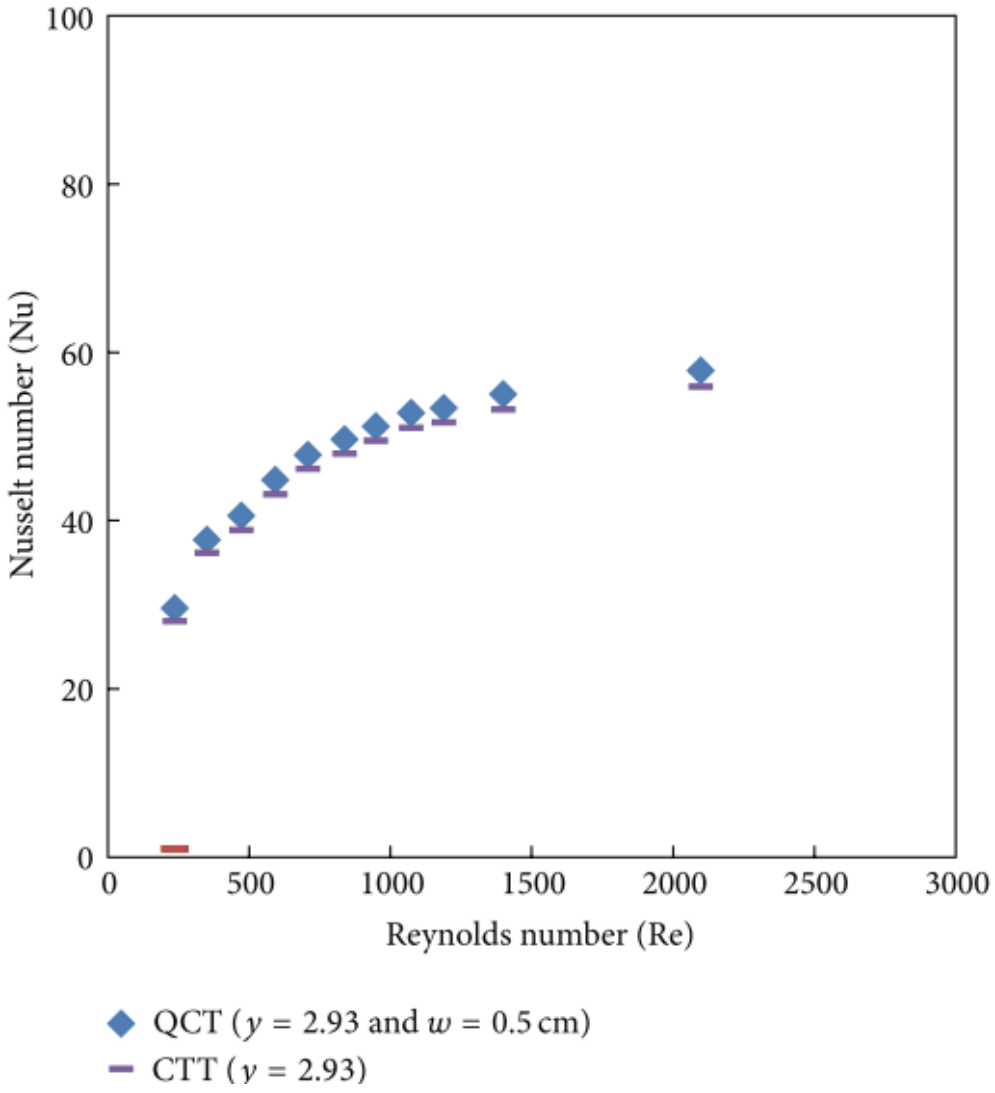

Figure 2.3 Effects of quadrant cut twisted tape configurations on the Nusselt number

Hasanpour *et al.* [22] reviewed the effects of various types of twisted tapes inserts on overall heat transfer coefficient enhancements of turbulent flow heat exchangers. This review showed that all shapes of twisted tapes produced increases in heat transfer than pressure drops and all of them can be used in heat exchangers. More concise this review showed that the twin and the helical screw

twisted tape inserts can reach the highest value among the other type of inserts. Mokkapati and Lin [23] investigated gas to liquid heat transfer performance of concentric tube heat exchanger with a twisted tape inserted corrugated tube and to evaluate its impact on engine performance and economics through heat recovery from the exhaust of a heavy-duty diesel generator. They concluded that the twisted tape insert causes a significant improvement in heat transfer performance of the plain tube heat exchanger and the corrugated tube heat exchanger improves the rate of heat transfer up to 82% and 35% when compared with the plain tube without and with twisted tape, respectively. The heat transfer rate in a corrugated tube heat exchanger with twisted tape insert is 67% more than that of corrugated tube without the insert. When the same twisted tape is inserted in the plain tube heat exchanger, the heat transfer rate is about 35.3% more than that of plain tube.

Effects of multiple tape inserts on heat transfer and pressure drop in a circular tube were investigated experimentally by Vashistha et al [24]. Their experiments were performed with tape inserts having twist ratios of 2.5, 3, and 3.5, and varying the Reynolds number ranges from 4000 to 14000. The counter-swirl twisted tapes with the twist ratio (y/w) of 2.5 produced the higher enhancement in the heat transfer and friction. The heat transfer and friction registered 2.42 and 6.96 times over a smooth tube, while the maximum value of the thermo-hydraulic performance factor was found to be 1.26. Nusselt number and friction factor values increased by decreasing the y/w of twisted tapes irrespective of the change in the Reynolds number. The counter-swirl type of twisted tape inserts presented higher heat transfer and friction in comparison to the co-swirl twisted tape inserts. Kumar *et al.* [25] used a solid hollow circular disk as an insert to investigate experimentally its effects on thermal performance and fluid flow characteristics in the heat exchanger tube. Their experiments were employed in the range of Reynolds number from 6500 to 23,000. It was observed that increasing the values of the diameter ratio increases significantly the thermal performance factor maximum value obtained at a diameter ratio of 0.8.

Kumar et al. [26] proposed a new design of multiple twisted tape inserts as a heat transfer augmentation device. It was assumed that the degree of turbulence near-wall tube can enhance by. The experiments were performed using multiple squares perforated with square wing twisted tape with different wind depth ratio and a stream parameter range 5000–27,000, where air was used as the working fluid. They resulted that the highest enhancement in Nusselt number and friction factor

was observed to be 6.96 and 8.34 times over plain circular tube. Correlations were developed for Nusselt number *Nu*, friction factor *f*, and thermal-hydraulic performance Nu, f, and η_p as functions of twisted tape and stream parameters. Deviations between predicted and experimental values for the three correlations were of the order ± 5.5%, ± 4.0%, and 6.0% respectively. Halim et al [27]completed an experimental and numerical study of utilizing ribs in a triple tube to enhance the cooling parameters. The effects of mass flow rate in tubes, temperature, height, and pitch of the rib and flow pattern on the heat transfer, performance index Nusselt number and friction losses were investigated. The results showed that the heat transfer coefficient increased by 15.7% and pressure drop by 47.4%. By reducing the triple tube rib pitch as illustrated. Guan et al [28] applied for a review on the performance evaluation of natural draft dry cooling towers and possible improvements via inlet air spray cooling. To characterize these varied spray patterns, the corresponding flow rate, pressure, mean droplet size, and droplet size distribution should be quantified. The influencing parameters are stated to determine a specific spray pattern. Furthermore, the governing equations controlling the droplet evaporation process are also compared based on their assumptions and conclusions. Lastly, the evaporative cooling involved in the pre-cooling system is firstly described mathematically. Then literatures are presented to evaluate the performance of the pre-cooling system. Their results illustrate that the inlet air pre-cooling would improve the efficiency of natural draft dry cooling tower and thus reduce power generation loss under high-ambient conditions.

Esfahani and Languri [29] studied the exergy performance of a shell-and-tube heat exchanger using graphene oxide Nano-fluids (NFs) experimentally. Graphene oxide particles were fabricated chemically and then characterized. The graphene oxide NFs were prepared at 0.01 and 0.1wt. % concentration, and thermal conductivity and rheological behavior of each sample were measured at 20 and 40 ºC temperatures. It was concluded that the increase in the concentration of graphene oxide particles resulted in higher viscosity and aggregate size in NFs at room temperature. The 0.01 and 0.1wt. % graphene oxide NFs showed about 9% and 20% higher thermal conductivity compared to distilled water at 25 ºC, respectively. Different parameters such as effect of NFs concentrations, temperatures, and flow rates of exergy destruction were investigated experimentally. Figure 2.4 shows a comparing the exergy loss of graphene oxide NFs to distilled water (DI) and graphene oxide (GO) showed that distilled water caused 22% and 109% higher exergy losses when compared to NFs at 0.01 and 0.1wt. % concentrations in laminar conditions,

respectively. It was also noted that at both laminar and turbulent flow regimes, exergy loss increased with the increase of hot fluid inlet temperature mainly due to the higher temperature differences between hot and cold fluids.

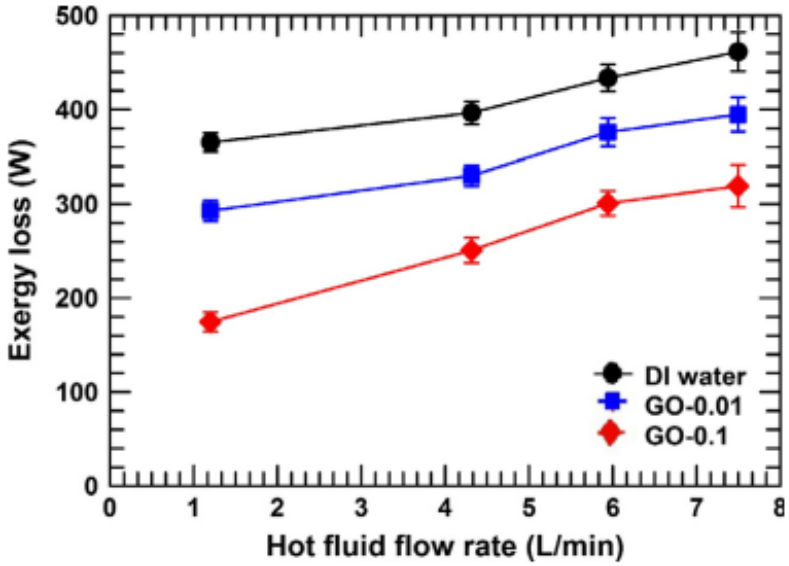

Figure 2.4 Exergy losses versus the hot fluid rate

Omara et al [30] studied the effects of versions of helical coil pitch and cross-section of the coil in the elliptic tube on heat transfer and pressure drop features for Reynolds Number range from 11103 to 33750. The smooth elliptic tube increased the efficiency of cooling (η) by about 5% comparing to the smooth usual circular. It is indicated that the Nusselt number (Nu), friction factor (f), and efficiency (η) enhanced by decreasing the pitch of inserted helical coils. The rectangular cross-section of the helical coil leads to an increase (Nu), (f) and (η) by 15%, 3%, and 14% respectively, comparing to the circular section.

Effects geometrical features of delta-wing (T-W) tape inserts on performance (Nu, f, and f_{THP}) of a double pipe heat exchanger were studied by Wijayanta *et al.* [31]. Inserts were placed in the inner tube with different wing-width ratio (i.e. 0.31, 0.47, and 0.63) and varying Reynolds number in the range 5300-14500. The T-W tape insert with a wing-width ratio of 0.63 produced the highest Nusselt number. The average increase in Nusselt number, friction factor, and thermal performance was recorded to be 77%, 1060%, and 15%, respectively when compared with the plain heat exchanger. Two correlations for the Nusselt number and friction factor were proposed based on

the experimental data obtained from this study. Bazgir et al.[32]performed a numerical study in the vortex tube refrigerator to predict the hydraulic and thermal features and the simulation results were verified and compared with the previous investigational results. It is predicted that the temperature difference between the inlet and outlet of the tube increased with cooling the outer surface of the tube so that the thermal efficiency enhanced. The temperature differences between the inlet Tin and outlet Tc of tube side versus the cold water mass flow for different length to diameter ratio (L/D) are investigated in Figure 2.5. The cooling efficiency and air temperature difference increased by 5.8 to 10.6% and 6.3 to 10.3%, respectively with vortexes and cooling water comparing with plain tube without water cooling.

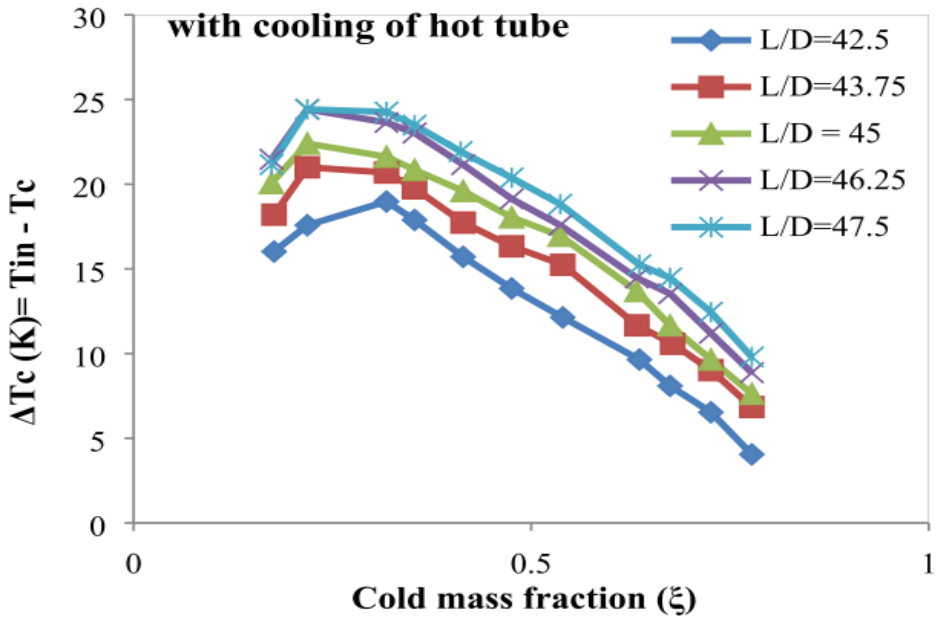

Figure 2.5 The temperature difference versus the cold mass fraction

Cui et al [33] finished a review to provide an inclusive account on recent progresses in evaporative cooling technologies, with a focus on enhanced evaporative cooling assisted by desiccants, membranes, or the combination of desiccants and membranes. The results showed that a novel approach was proposed in this review to classify these emerging different enhanced evaporative cooling technologies. Enhanced pre-treatment evaporative cooling ambient air using membranes, desiccants, or a combination of membranes and desiccants to significantly increase cooling

efficiency and minimize side effects associated with high moisture and, in some scenarios, cross-contamination inherited from ambient air evaporative cooling. By studying these enhanced technologies for evaporative cooling, smaller hybrid heating, ventilation, and air conditioning devices for buildings or mobile cooling devices for smaller space cooling or microclimate cooling can grow. Jeong et al[34] studied a method to increase the heat coefficient by utilizing small protrusion with crescent shape as vortexes generator in a dimpled channel at a constant Reynolds number equal to 2800. It is indicated that the thermal performance factors, such as fanning friction factor f/f_o, Colburn j factor j/j_o, and volume goodness factor G_v/G_{vo} were increased by 21%, 11%, and 4%, respectively with the new modification. Khorasani et al.[35] investigated the effect of spiral wire diameter and pitch on the thermal and hydraulic performance of a helical tube under constant heat flux. They finished the tests through four different configurations with varying the pitches, diameters, and airflow rates. It is specified that the heat transfer and pressure drop increased with an increase of wire diameter and a decrease of the pitch. Nu Nusselt number enhanced with the rise of both spring pitch and wire diameter. Qin and Wang [36] studied thermal and hydraulic features of sodium-potassium allay NaK in a helical wire wrapped annulus numerically. It was established that the Nu and pressure losses increased by 15% and 17%, respectively with the helical wire. The thermos-hydraulic performance ratio achieved the values between 0.92– 0.99 with high mass flow rates. Sayed et al.[37] studied the heat transfer and pressure drop performance with three configurations of rectangular copper alloy woven wire mesh is in tubes. It is indicated that the wire mesh enhances the heat transfer coefficient with low cost and simple manufacture. The results showed that the Nusselt number and pressure drop increased with the wire mesh as the same tend of previous studies as seen in Figure 2.6 where many wire mesh with different diameters and previous studies were investigated.

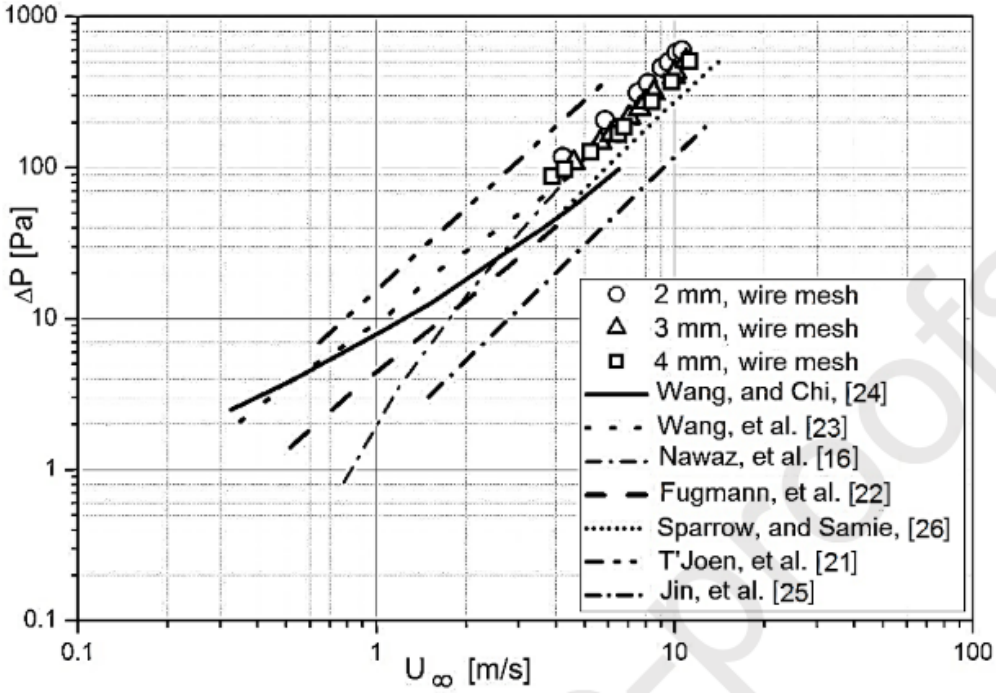

Figure 2.6 The pressure drop versus the velocity for wire mesh and previous studies

Song et al [38] studied exergy destruction and exergy flow in direct contact process between humid air and water as a liquid phase desiccant solution theoretically. The equivalent air film of water or a solution is a medium not only for the transfer of heat and mass but also for exergy and is thus used to determine the supplied exergy or obtained exergy of the water/solution. The solution's concentration exergy may be defined as the difference in exergy between the two equivalent air films. Wet air provides its thermal exergy and humid exergy, which flows through the equivalent air film, except for the exergy destruction portion, during direct evaporative cooling between humid air and water. Then, the rest all become the thermal exergy of the water. The previous processes are inverted in the dehumidification of condensation. The solution provides the thermal exergy and concentration exergy while dehumidifying between humid air and solution to complete the exergy flow from solution to water. In the regeneration process, except for the exergy destruction portion, the humid exergy supplied by humid air is divided into two parts: one becomes the solution's concentration exergy, and the other is transformed into the solution's thermal exergy.

Liu et al [39] examined the heat transfer rates and flow features in the parabolic duct. It is indicated the curve line of temperature difference distribution is straight and linear compared to the

trapezoidal one. As a result of this, the heat transfer efficiency and heat coefficient increased. Nakhchi et al [40] studied the effects of single and double novel perforated louvered strip inserts on heat coefficient and thermal index factor with turbulence flow with range of the Reynolds number form 5000 to14000 numerically. The tests were completed with a slant angle variation from 15° to 25° and compared to the rounded pipe and conventional louvered strip inserts. It is revealed that fluid flow mixing between the wall boundaries and center core area increased with the axial velocity in the case of θ =25°. Rahmati and Gheibi.[41] studied the effects of fins with tubes of the hot water radiator numerically and experimentally. It was decided that the new modification of the fin increases the heat transfer surface and the output heat by 50% and that leads to save energy in the whole buildings.

Jafarzad and Heyhat [42] introduced the thermal and exergy analysis of air- nanofluid bubbly flow in a double pipe heat exchanger. Around the same time, air bubble injection and nanofluid were applied to boost the transmission of thermal energy. Results indicate a promising potential in performance enhancement of the combined method.

2.2 THE NOVELTY OF THE STUDY

As seen from previous literature, many studies investigated heat transfer and friction factor parameters in case of utilizing twisted tape, or helical tape or helical wire to enhancing the cooling in tubes. But fewer papers studied the effect of spring wire in tubes on thermal and exergy parameters. Many studies used the insets only inside the tubes. In this paper, the study of the effect of multi-spring wire on heat transfer, friction factor, and exergy losses numerically. This study aims to increase the cooling of air in tubes as application of air conditioning. The thermal parameters such as Nusselt Number and heat flux and hydraulic performance like friction factor and exergy efficiency will be studied for a range of Reynolds number from 2800 to 18000.

3. NUMERICAL STUDY

In this chapter, the physical model that was achieved by SOLIDWORKS will be introduced. Meshing generations, governing equation and data reduction will be presented

3.1 TUBE MODEL

The drawing of hot air cooling inside the tube by cold water is illustrated in Figure 3.1 where, the hot air inlet the tube with constant temperature at 80 ºC, and the cold water inlet temperature equals 27 ºC. More specifications are in Table 3.1

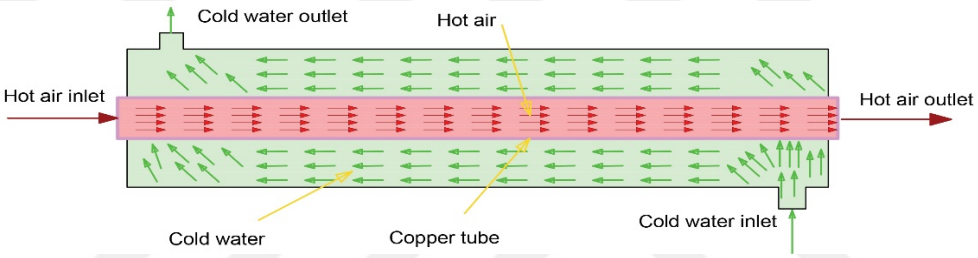

Figure 3.1: Schematic view of hot and cold fluid inlets and outlets in the heat exchange

Table 3.1: Properties of hot air and cold water

Properties of hot air		Properties of cold water	
Temperature inlet	80 ºC	Temperature inlet	27 ºC.
Density	1.225 kg/m^3	Density	998 kg/m^3
Specific heat	1006.43 J/kg.ºK	Specific heat	4182 J/kg.ºK
Reynolds number range	2800 to 18000	Reynolds number `	18000

SOLIDWORKS program [43] was used to draw the domains of hot air inside the tube, cold water outside the tube and copper tube as seen in Figure 3.2. The properties of tube that is utilized in the numerical simulation is given in Table 3.2.

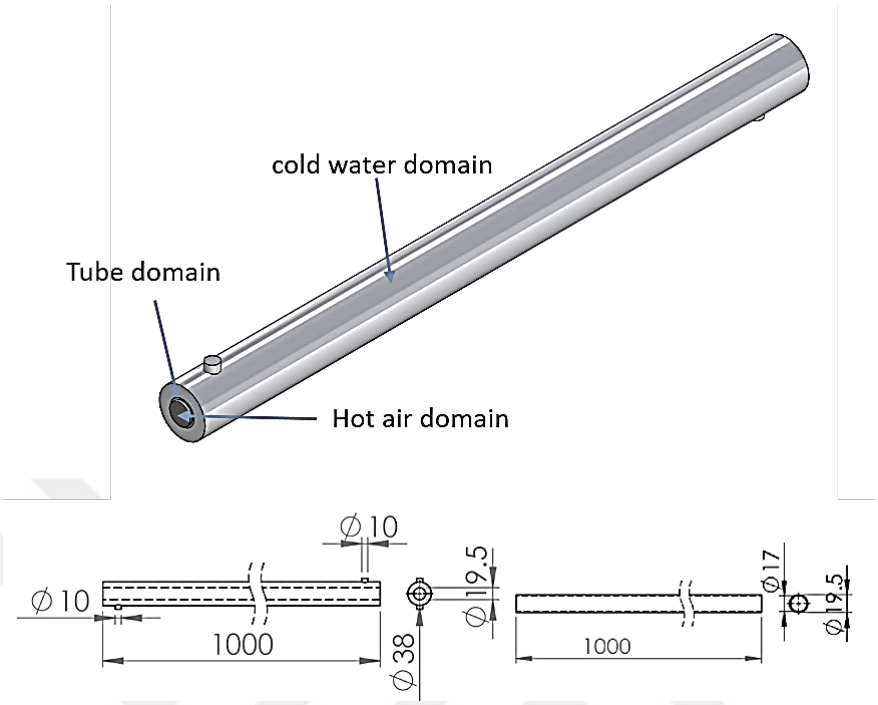

Figure 3.2: Three dimensions domains and dimensions of hot air, cold water and a tube by SOLIDWORKS

Table 3.2: Tube specifications used in simulation

Tube specifications	
Length	1000 mm
Inner diameter	17 mm
Outer diameter	19.5 mm
Material	Copper

3.2 SPRING SPECIFICATIONS

The spring length is 998 mm and the spring pitch equals 50 mm where the diameter of spring is 2 mm and it is fabricated from carbon steel. Three configurations are utilized in this study: single spring, double spring, and three spring inserted in tube to investigate the thermal and hydraulic performance of air cooling in tubes. Figure 3.3 shows the elevation view of spring configurations:

single spring, double spring, three springs, four springs, and five springs where there is no contact between the springs inside the tube. Spring specifications are shown in Table 3

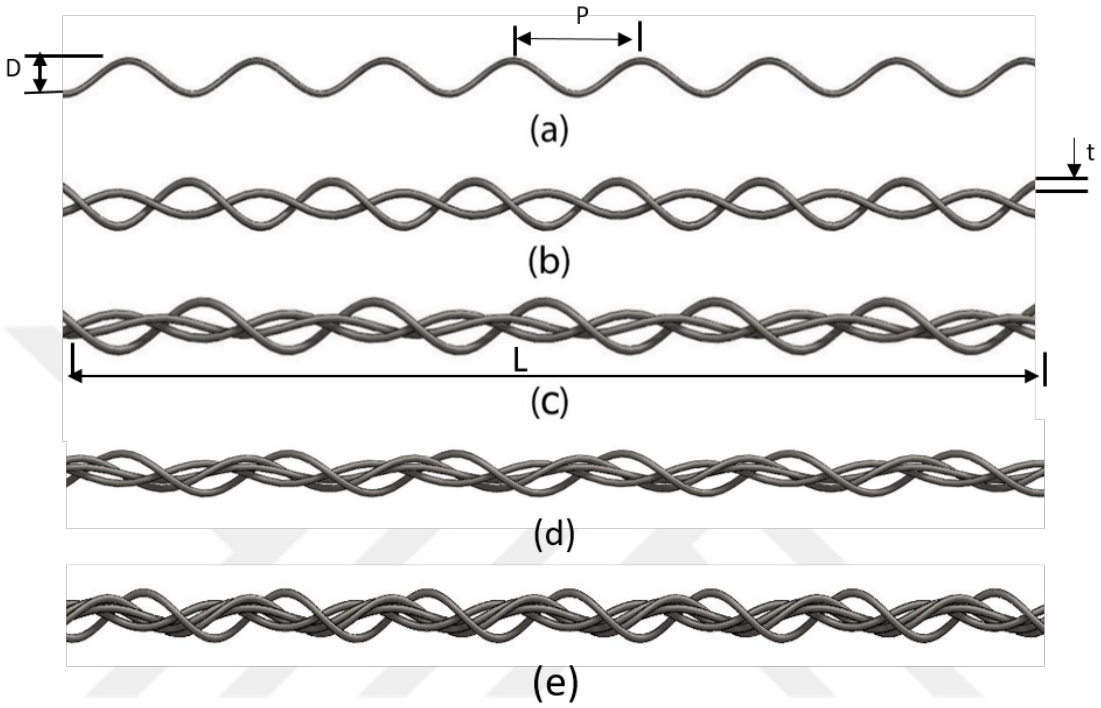

Figure 3.3: Elevation view of spring configurations (a) single spring (b) double spring (c) three springs (d) four springs (e) five springs

Table 3.3: Spring specifications

Spring specifications	
Length (L)	998 mm
Outer diameter of helical (D)	15 mm
Pitch (P)	50 mm
Wire thickness (t)	2 mm
Material	Steel

Figure 3.4 indicates the 3D view of spring configurations: single spring, double spring and three springs, four springs, and five springs. It is indicated that all springs have the same length, pitch so that the effect of multi springs inside the tube will be showed and compared with the single spring.

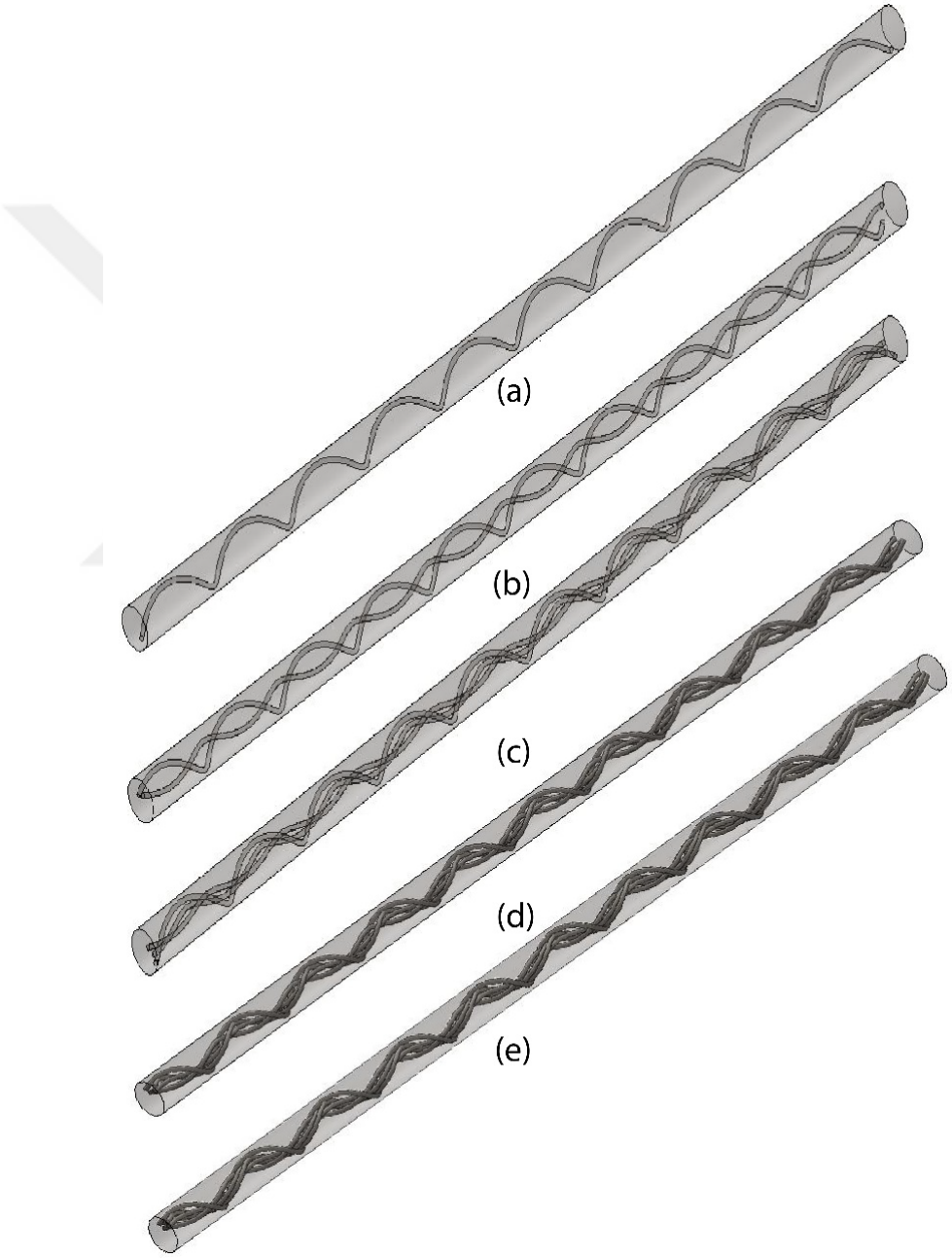

Figure 3.4: Three dimensional view of spring configurations (a) single spring (b) double spring (c) three springs (d) four springs (e) five springs

3.3 WIRE DIAMETER CONFIGURATION

Figure 3.5 shows the three spring wire diameters configuration (1mm , 2 mm , 3 mm) that were utilized for determine the optimum wire diameter where the pitch length is constant at 50 mm .

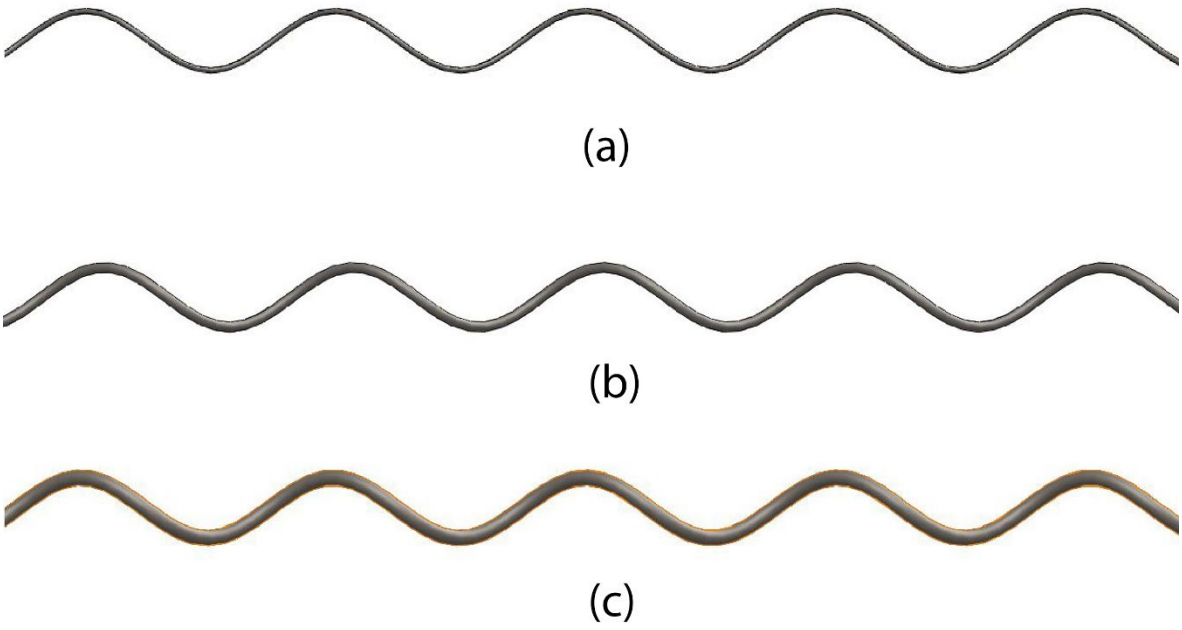

Figure 3.5 Spring wire diameter configurations (a) t=1 mm, (b) t=2 mm, (c) t=3 mm

3.4 PITCH LENGTH CONFIGURATION

Figure 3.6 shows the pitch length configurations utilized in the simulation tests to indicate the optimum spring pitch length at constant diameter t=3 mm. Heat transfer and pressure drop parameters will be indicated to show the optimization condition.

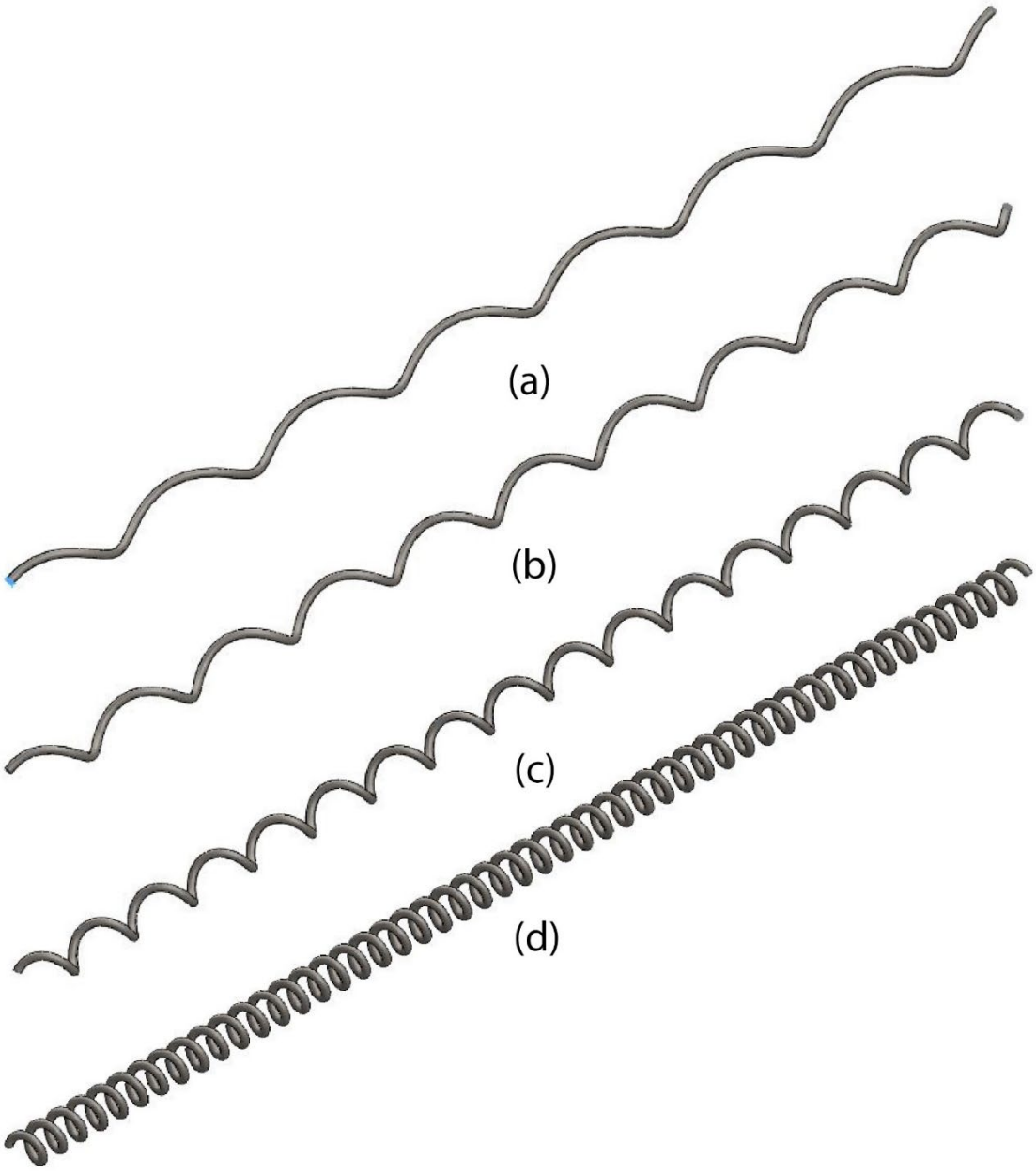

Figure 3.6 Spring pitch length configurations (a) P=70 mm, (b) P=50 mm, (c) P=30 mm, (d) P=10 mm

3.5 GRID GENERATION

The grid generation is performed by ANSYS fluent software Figure 3.7 and Figure 3.8 shows the grid distribution in the three domains and side view with a 3D view of the mesh utilized in the current numerical investigation. The radial direction in the direction of the U axis were, the axial direction in the Z direction. As can be perceived, inflation layers are used for mesh generation near

the walls of the copper tube. Hexahedron grid is chosen for grid generation the hot air inside the tube and tetrahedral grids are generated for cold water outside the tube. Three mesh conditions are used to check the mesh independence with 3986214, 5935221, and 6031452 numerical elements.

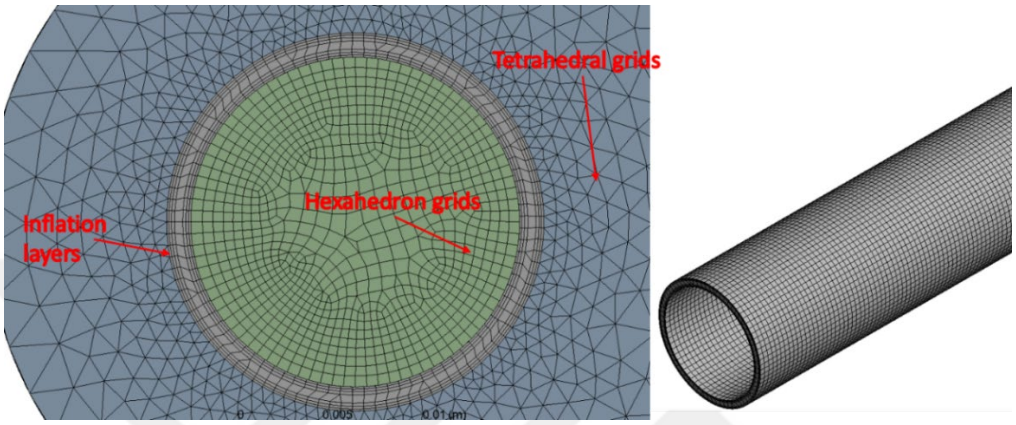

Figure 3.7: Grid generation in computational domains in side view and 3D view

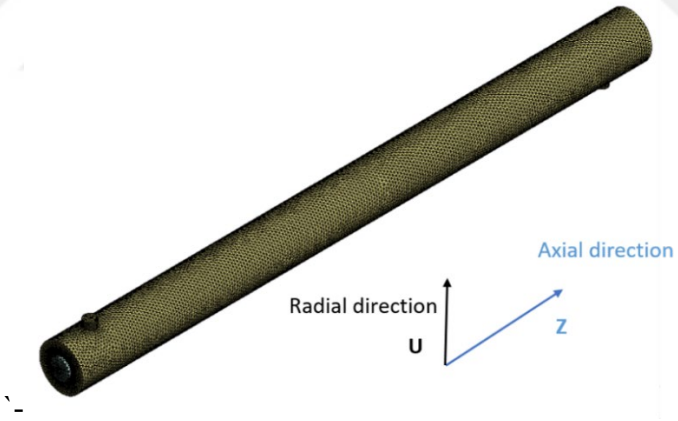

Figure 3.8: Meshing of the whole model in 3D view

The error in convection heat transfer coefficient and friction factor are tested in the cases of the three conditions and it is indicated the lowest error in all tests achieved with 6031452 elements as seen in Table 4 and no change in results with increasing number of elements after this condition so that this is used for this study.

Table 3.4: Error percentage of heat transfer coefficient

Meshing elements number	3986214	5935221	6031452
Convection Heat transfer coefficient	3.521%	1.92%	0.701%
Friction factor	2.21%	1.601%	0.421%
Exergy efficiency	1.31%	1.02 %	0.345%

3.6 BOUNDARY CONDITIONS

The numerical study was examined to designate the airflow pattern, temperature, velocity, and pressure cross the tube of the current configurations. Figure 3.9 shows the Boundary conditions of inlet and outlets of air and water as well as the walls were indicated precisely according to the previous and suitable conditions of the model. For the inlet of the hot air, temperate with constant value at 80 C^o is determined and velocity is chosen as a variable value so that the Reynolds number varies from 2800 to 18000 as the range of turbulence region as seen in Table 5. The cooling water inlet is selected as a constant mass flow rate and temperature at 27 ^oC so that no effect on the air cooling in the tube can be predicted with change the velocity of air. Both of cold water and hot air exits were supposed to be pressure outlet boundary condition with zero back pressure to predict the pressure losses in the tube side. The hot air -tube wall has been analyzed with heat transfer and convection where the wall of the cold water domain is considered to be with heat flux at zero value so that the domain is completely insulated. The CFD code was realistic for the realizable k-ε simulations stated in this study.

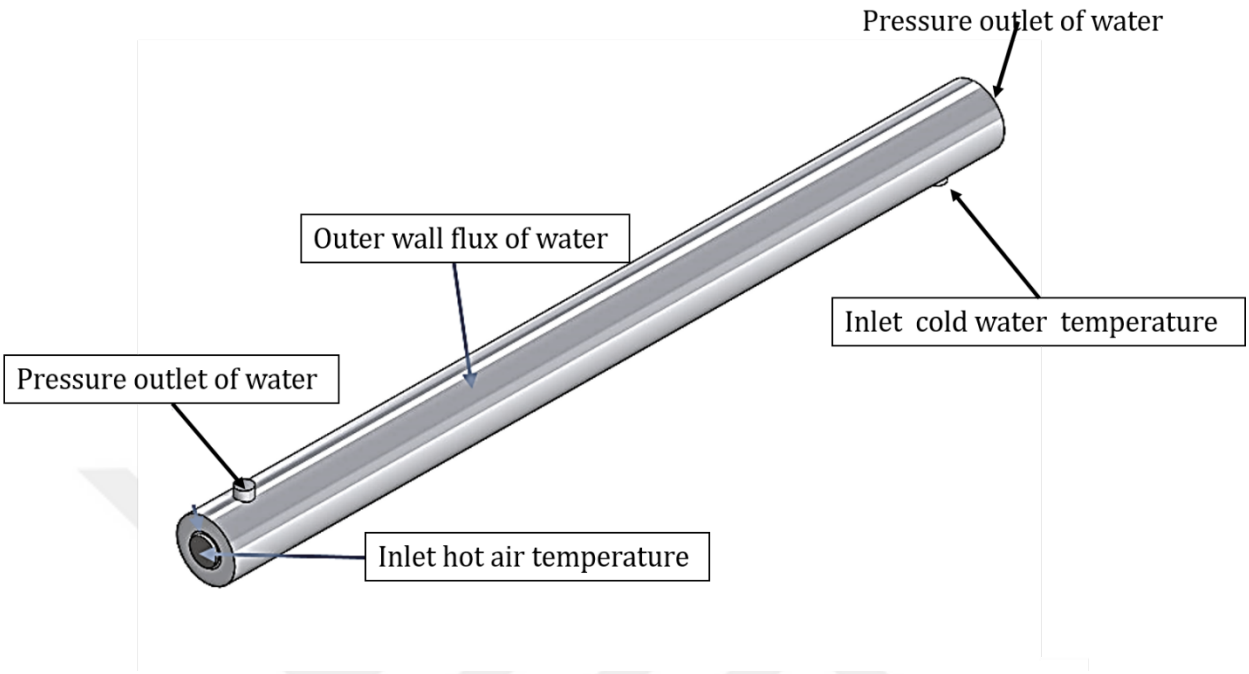

Figure 3.9: Boundary conditions for the numerical model

Table 3.5: Boundary conditions

Boundary conditions	
Inlet hot air temperature	80 ºC
Inlet cold water temperature	27 ºC
Pressure outlet of air	Atmospheric pressure
Pressure outlet of water	Atmospheric pressure
Outer wall flux of water	0.0
Range of Reynolds number	2800 to 18000

Finite volume method scheme is used to solve the base of the governing equation on this analysis. For convective-diffusive terms in the (RANS) equations, continuity and momentum equations. For the pressure-velocity coupling, the SIMPLE is utilized.

3.7 SIMULATION TESTS ARRAY

To determine the optimum choice for the number of springs, pitch length, and wire thickness, 14 numerical tests were achieved. Table 6 shows the required number of tests for performance optimization for air cooling inside tubes.

Table 3.6: Numerical tests array

Tests	Number of springs	Pitch length mm	Wire thickness mm	Water flow rate LPM
Number of springs effects				
1	0	50	2	1
2	1	50	2	1
3	2	50	2	1
4	3	50	2	1
5	4	50	2	1
6	5	50	2	1
Spring pitch length effects				
7	3	10	2	1
8	3	30	2	1
9	3	50	2	1
10	3	70	2	1
Wire diameter				
11	3	30	1	1
12	3	30	2	1
13	3	30	3	1
Water flow rates effects				
14	3	30	2	1
15	3	30	2	2
16	3	30	2	3

3.8 MATHEMATICAL FORMULATION

The heat transfer rate of hot air in the tube side that depend on the heat transferred from hot air to cold water can be expressed as:

$$Q_a = M_a C_{p.a}(T_{a.in} - T_{a.out}) \quad (3.1)$$

Where, M_a is the mass flow rate of air, $C_{p.a}$ is the specific heat of air and $T_{a.in}$ and $T_{a.out}$ are the inlet and outlet of air temperature, respectively. The heat transfer to cold water outer the tube can be calculated by:

$$Q_w = M_w C_{p.w}(T_{w.out} - T_{w.in}) = hA(T_{tw} - T_{ave}) \quad (3.2)$$

Where, M_w is the mass flow rate of cooling water, $C_{p.w}$ is the specific heat of water and $T_{w.in}$ and $T_{w.out}$ are the inlet and outlet of water temperature, respectively. The T_{ave} is the average temperature of hot air and T_{tw} is the average temperature of the external wall of tube:

$$T_{ave} = \frac{T_{a.in} + T_{a.out}}{2} \quad (3.3)$$

So that the average heat transfer coefficient can be calculated by:

$$h = \frac{M_a C_{p.a}(T_{a.in} - T_{a.out})}{A(T_{tw} - T_{ave})} \quad (3.4)$$

So that the Nusselt number can be calculated by:

$$N_u = \frac{h\, D_h}{K} \quad (3.5)$$

D_h is the hydraulic diameter and k is the thermal conductivity. The Reynolds Number can be determined by:

$$Re = \frac{V D_h \rho}{\mu} \quad (3.6)$$

Where, V , is the velocity and ρ is the density . Prandtl number is defined from this relation:

$$Pr = \frac{c_p \mu}{K} \quad (3.7)$$

Dittus and Boelter equation can be expressed in:

$$N_U = 0.023\, Re^{4/5} Pr^{.3} \quad (3.8)$$

The friction factor depends on the pressure drop and geometry of the tube and can be calculated by.

$$f = \frac{\Delta P}{\rho \frac{l}{D_i} \frac{V^2}{2}} \quad (3.9)$$

The exergy efficiency can be determined by [44]:

$$\eta_e = 1 - \left\{ \frac{T_o \left[M_a C_{p.a} \ln\left(\frac{T_{a.out}}{T_{a.in}}\right) + M_w C_{p.w} \ln\left(\frac{T_{w.out}}{T_{w.in}}\right) \right]}{M_a C_{p.a} \left[(T_{a.in} - T_{a.out}) - T_o \ln\left(\frac{T_{a.out}}{T_{a.in}}\right) \right]} \right\} \quad (3.10)$$

4. RESULTS AND DISCUSSIONS

In this section, description of the numerical model used in the simulation, mesh generation, governing equation that controls the process of heat and mass transfer, model validation according to the experimental set up and numerical results represented in temperature and velocity contours were studied.

In this section, the numerical model will be validated with the experimental results of studies [44, 45]. Then the numerical results will be introduced in the form of Nusselt number, heat flux, and friction factor, and exergy efficiency. The countors and streamlines of velocity, temperature, and pressures will be introduced to indicate the effects of the springs.

4.1 MODEL VALIDATION

Nusselt number for the plain tube was studied where the range of Reynolds number is between 2800 to 10000 where the numerical results of the plain tube were validated with Eiamsa-ard [44] with the same dimensions and conditions. Else the smooth tube results that indicated validated by calculation the parameters by equations of Dittus and Boelter [46]. **Figure 4.1** shows the relation between the numerical results and the previous results of Eiamsa-ard and Dittus and Boelter. It is indicated that the deviation between the results and is very limited. Therefore, the present numerical predictions have reasonable accuracy. The regular differences between numerical and previous results for Nusselt number are around 7.12%. The highest dissimilarity for Nusselt number is 11.94% and the smallest dissimilarity is 5.821%.

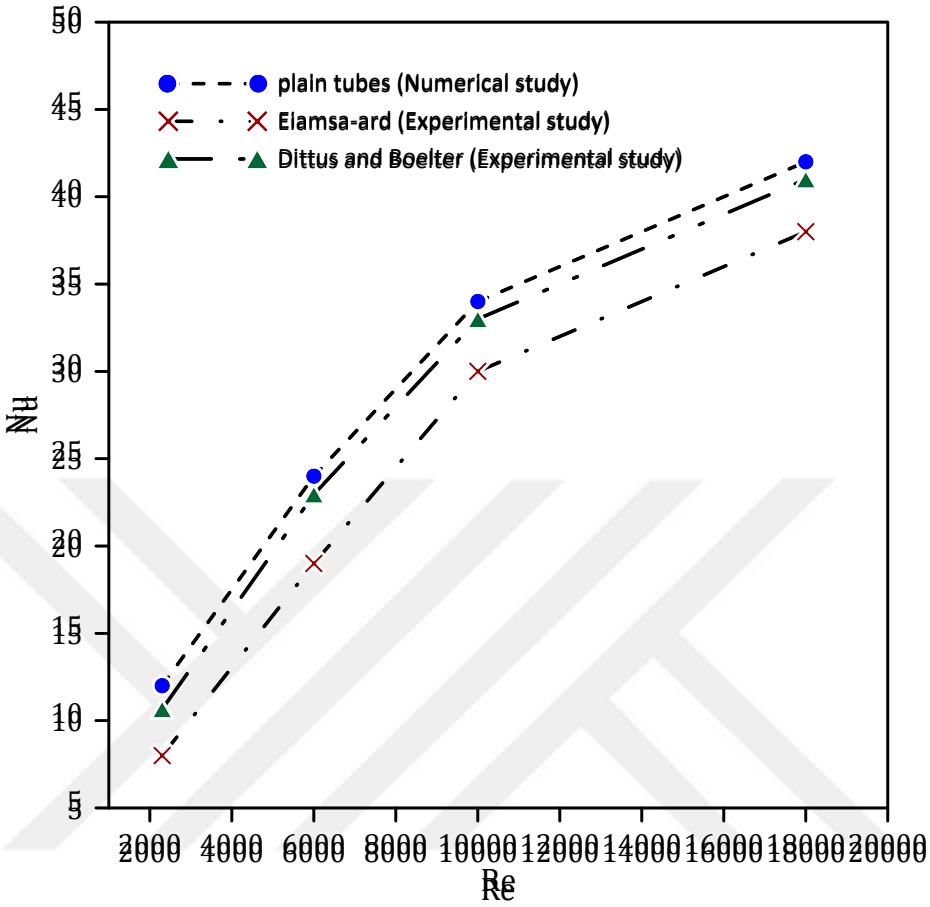

Figure 4.1 Validation of Nu number between the numerical results and the previous results of Eiamsa-ard and Dittus and Boelter

Moreover, Figure 4.2 shows the validation of the friction factor between the numerical results and the previous results of Eiamsa-ard and Darcy. The validation results explained that the differences between the numerical and the experimental results are acceptable where the regular differences between numerical and previous results for friction factor are around 5.31%. The highest dissimilarity for Nusselt number are 7.311% and the smallest dissimilarity is 3.41%. In general, the differences are acceptable for simulation errors and these errors for modeling is effective and accurate in this study.

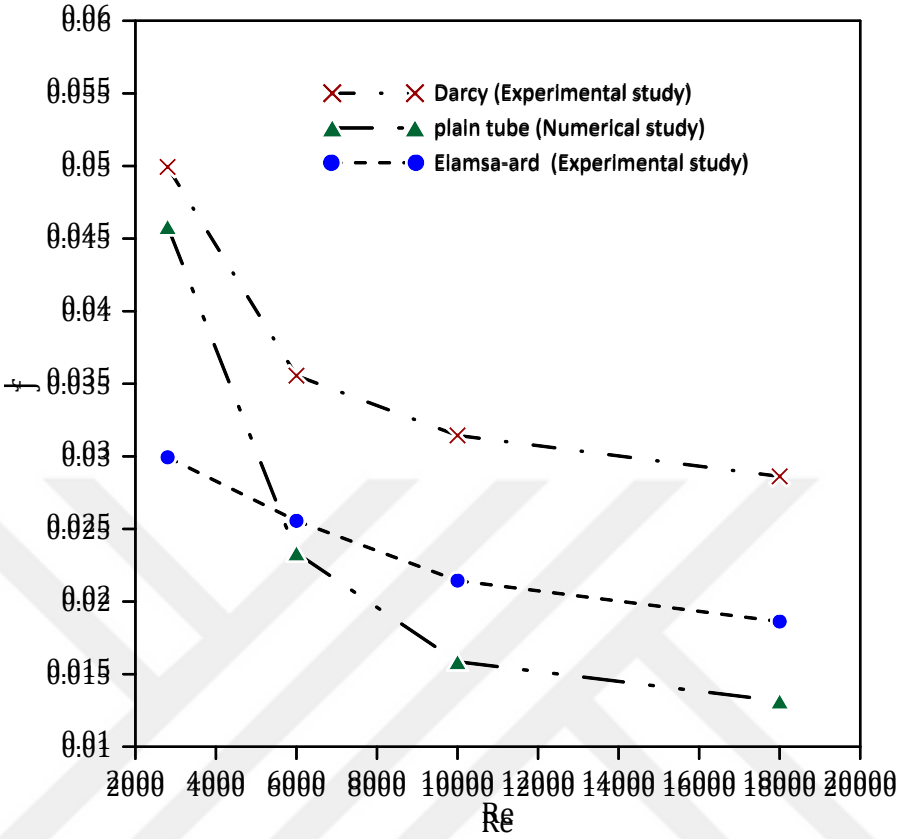

Figure 4.2 Validation of friction factor between the numerical results and the previous results of Eiamsa-ard and Darcy

4.2 OPTIMIZATION OF THE NUMBER OF SPRINGS INSIDE THE TUBE

4.2.1 Nusselt Number

It is indicated that Nusslet number increase with the rise of Reynolds number where the Reynolds change from 2800 to 18000 to achieve the fully developed region as seen in Figure 4.3, four springs configuration have the highest Nusslet number following the figure of 65 to 80. It is defined that a spring inserted in the tube increased swirl flow with secondary air mixing flow and radial pressure gradient. The boundary layer along the tube wall would be thinner with the increase of radial swirl and pressure. It is indicated that the Nusslet number achieved the value of 12 without spring at the lowest Reynolds number where the single, double, three springs achieved the figures of 43, 58, and 64, respectively. The Nusslet number achieved value around 40 without spring at

the highest Reynolds number where the single, double, three, and five springs achieved the figures of 70, 76 and 81, and 89, respectively. In the case of five springs, the Nusselt number is smaller than the configuration of four springs as the cross-section area decreased greatly and that affects the amount of air goes through the tube. That can explain the reduction in the heat transferred to the cold water. The effect of the multi-springs decreased at low Reynolds numbers because of the weak swirl and low flow velocity. Thus, the increase in Nusselt number was low at smaller Reynolds number, while it became greater at the higher Reynolds numbers.

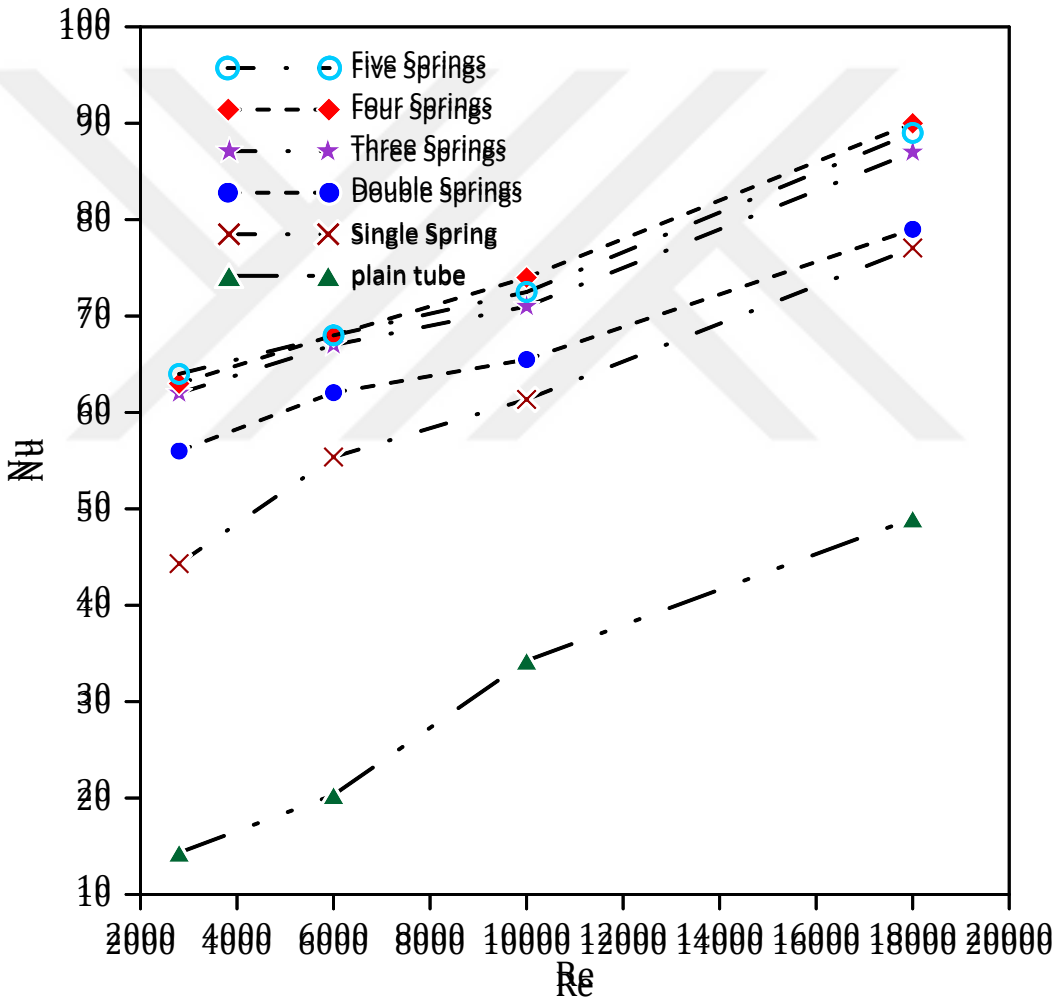

Figure 4.3 The relation between the Nusslet numbers versus the Reynolds number for various springs

4.2.2 Heat Flux

Figure 4.4 shows the relation between the heat fluxes versus the Reynolds number for various springs where the heat flux enhanced with the increase of Reynolds number. The four spring's configuration has the highest heat flux following the figure of 322 to 399 W/m^2. The heat flux for the five spring is less than the four springs at the high Reynolds number as adding five springs decreases the cross-section area so that the fluid has less time in the tube. It is can be explained as the heat transferred easily through the flow and swirl cause flow to be turbulent which leaded to even better convection heat transfer. Enhancement of the heat flux can be explained as the increase of the values of heat transfer coefficient and the temperature difference between wall and average fluid ($T_{tw} - T_{ave}$) significantly decreased for the tube with the springs.

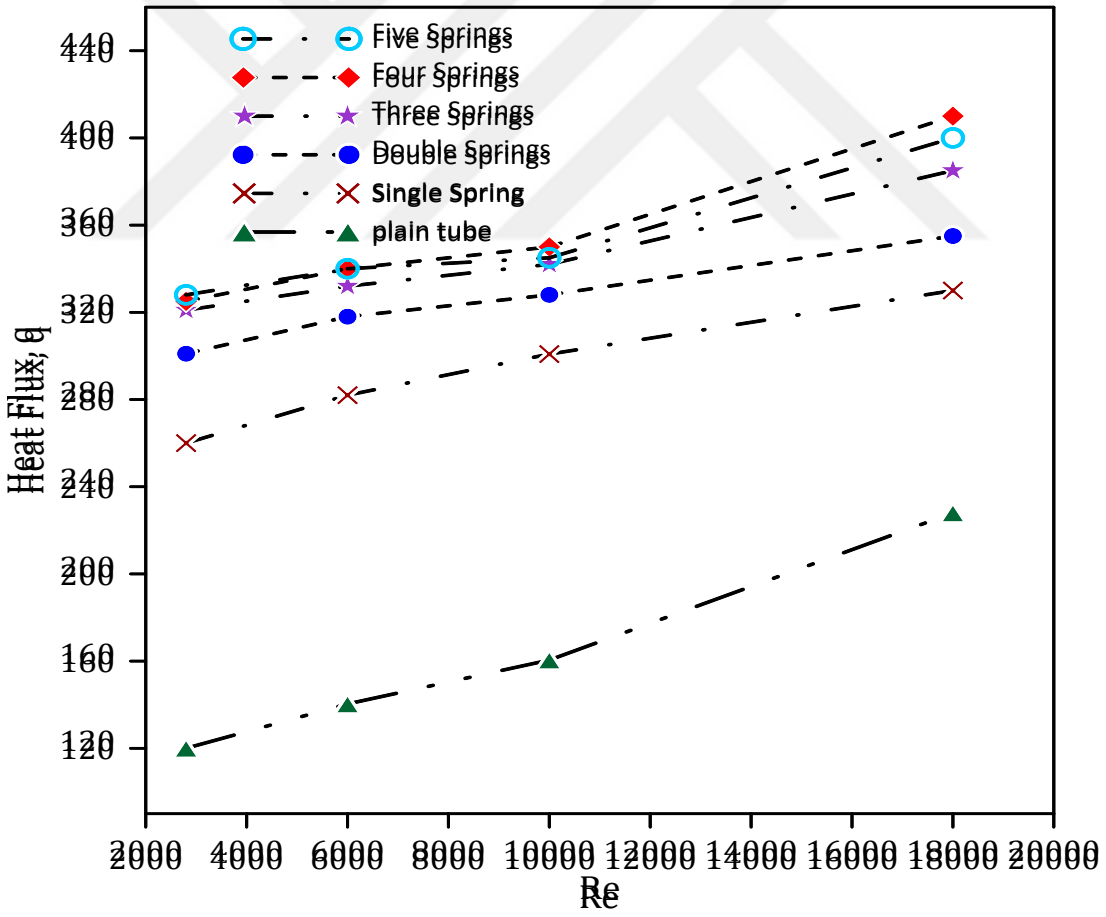

Figure 4.4 The relation between the heat fluxes versus the Reynolds number for various springs

4.2.3 Friction Factor

Figure 4.5 investigates the relation between the friction factors versus the Reynolds number for various springs. The friction factor decreases with the increase of Reynolds. Five springs achieved the highest friction factor from 0.1 to 0.25 comparing to other configurations and pain tube. It can be seen that the friction factor was in the similar trend for both the plain flow and the spring insert and the friction factor of the spring insert was higher than that in the plain tube. It is known that the increase of friction factor influences the performance badly so that the decrease of friction factor is better to save energy in the pumping system. It can be noticed that the relation between the heat transfer enhancement representing in Nusselt number and pressure drop representing in friction factor is the most fundamental parameter for the optimization process. So that four springs can be chosen as the optimum number as it achieved the maximum Nusselt number with suitable friction factor.

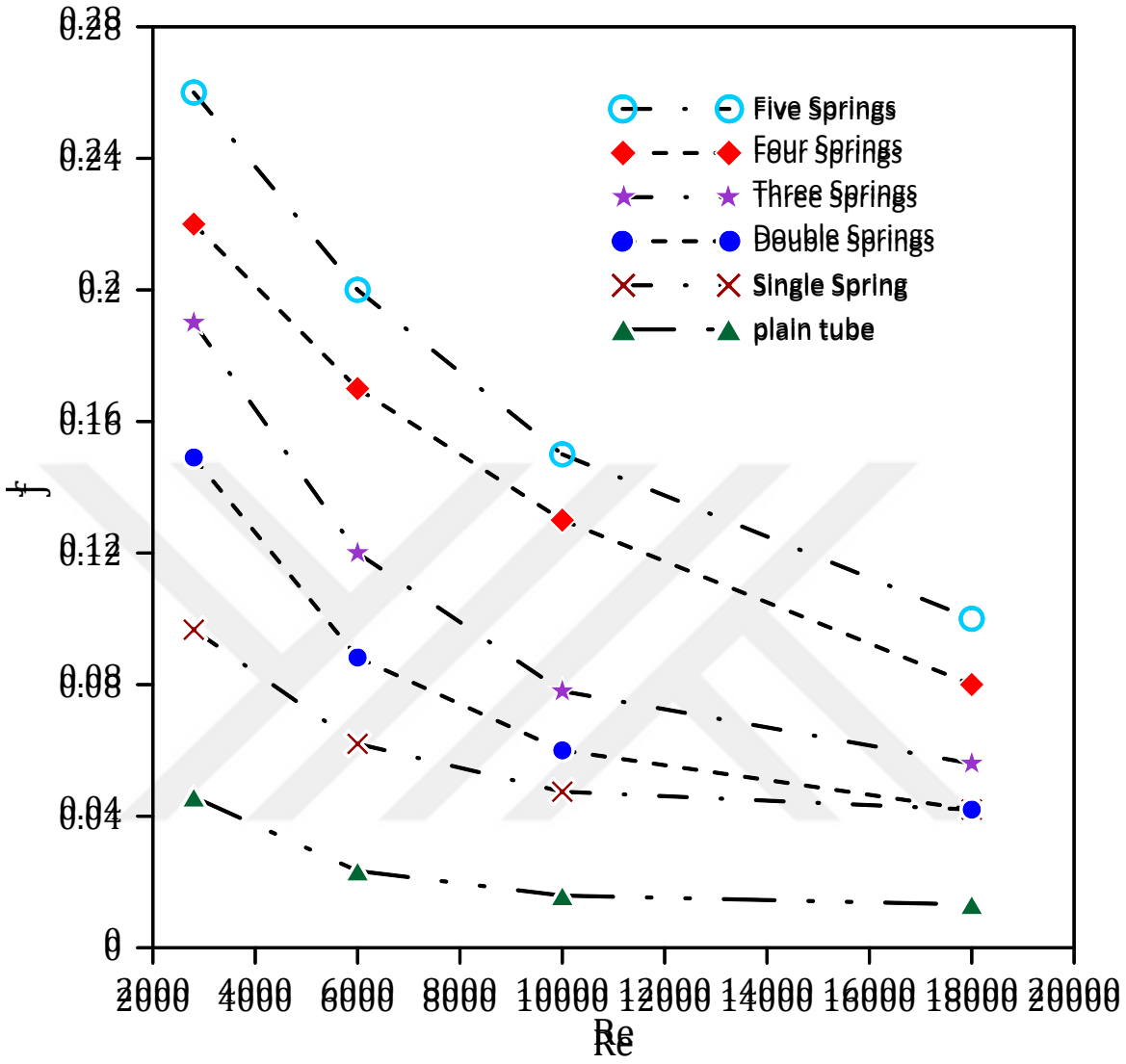

Figure 4.5: The relation between the friction factors versus the Reynolds number for various springs

4.2.4 Exergy Efficiency

Exergy is the extreme sum of work that can be attained theoretically with a reversible process in which complete equilibrium with the environment is reached. The reference environment conditions is known to compute exergy where the temperature of the reference environment that is named ambient temperature in this study is constant at 27 ºC. Exergy efficiency of the air in the tube as illustrated in Figure 4.6 versus Reynolds number where the exergy efficiency increased with the rise of the Reynolds number. The exergy efficiency increase with the Reynolds number

and the higher the number of springs in the tube, the higher the value of the exergy efficiency so that the four spring has the maximum value of the exergy efficiency comparing to other configurations in this study. The heat flux for the five spring is less than the four springs at the large number of Reynolds, as the addition of five springs reduces the area of the cross section so that the fluid has less time in the tube. On the other hand at the Reynolds number the five springs increase turbulence with more time cross the cooling tube.

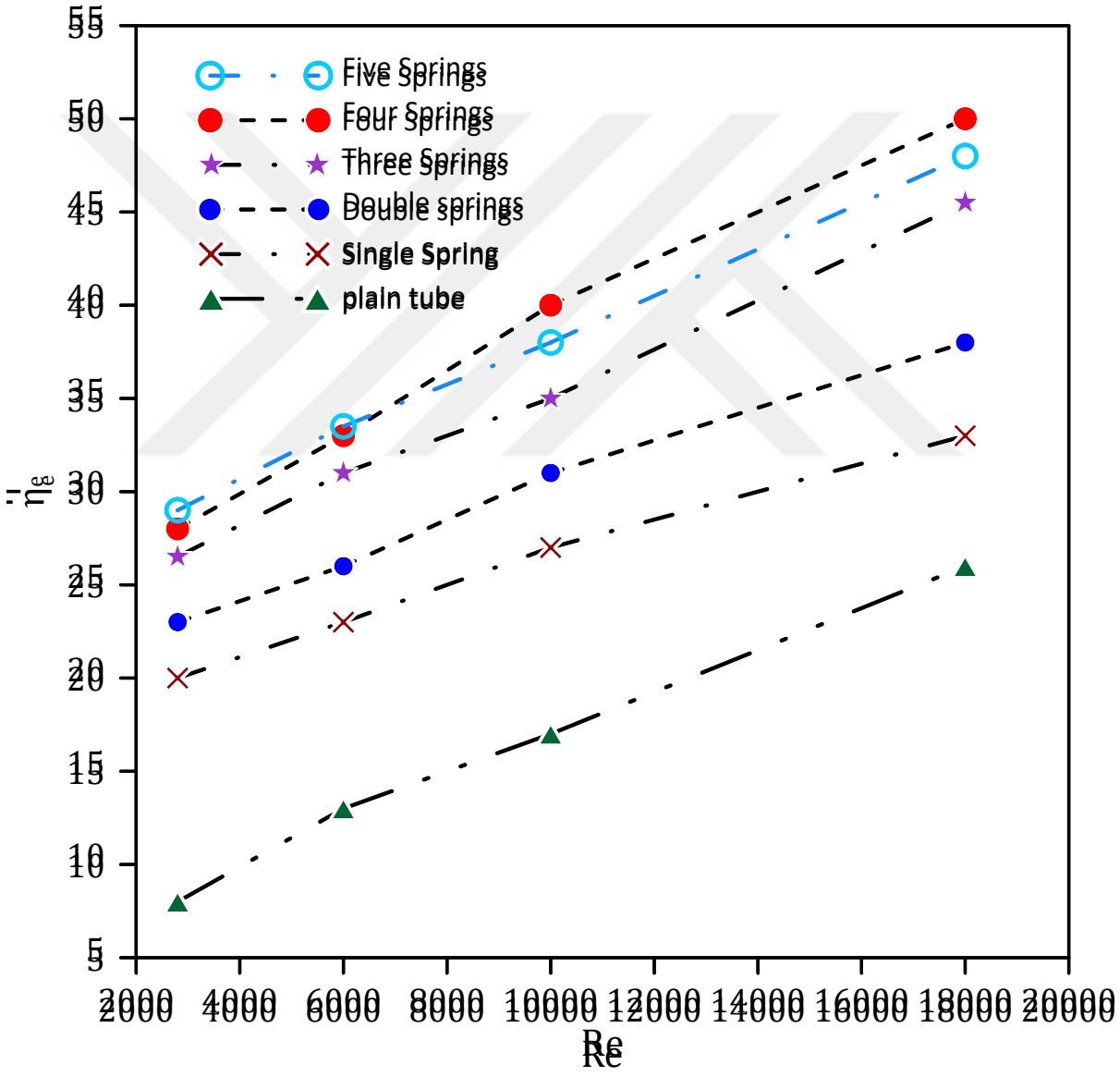

Figure 4.6: The relation between the exergy efficiency versus the Reynolds number for various springs

4.2.5 Temperature Distribution

Figure 4.7 shows the temperature distribution of hot air and cold water cross-section of the tube for a plain tube and all configurations. It can be seen that the hot air temperature decrease in the tube side was, the cold water temperature increase in the outer domain. The temperature grade close to the wall becomes smaller, especially in the case of four springs. The dissimilarity inclinations of the flow and temperature fields agree well. Spring inside the tube increases the disturbance of the boundary layer so that the heat transfer enhanced.

4.2.6 Velocity Components

The velocity of hot air investigated in Figure 4.8 where the springs inside tube lead to increase the mixing between the boundary layers and force the air to change the directions so that the swirling in the tube enhanced. This can be noticed in figure 4.8.a were no spring inserted, the streamlines of the velocity have parallel lines. In figure 4.8.b to figure 4.8.e, it can be seen that the streamlines of velocity have dissimilar lines, there is mixing between the lines and swelling increase gradually with increase the number of the springs.

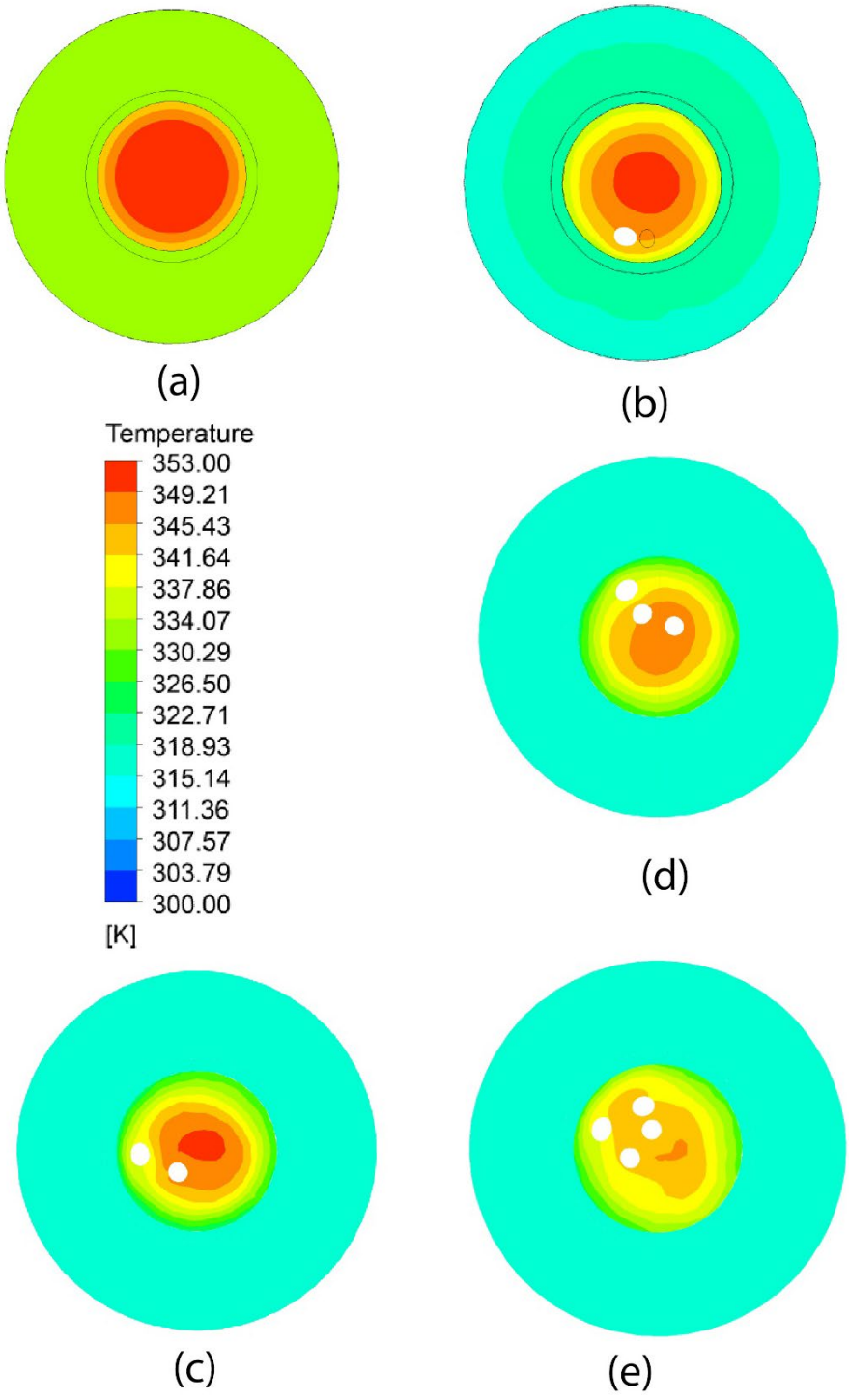

Figure 4.7 Temperature distribution of hot air and cold water for cross section of the half of the tube (a) plain tube, (b) single spring, (c) double spring, (d) three springs, (e) four springs

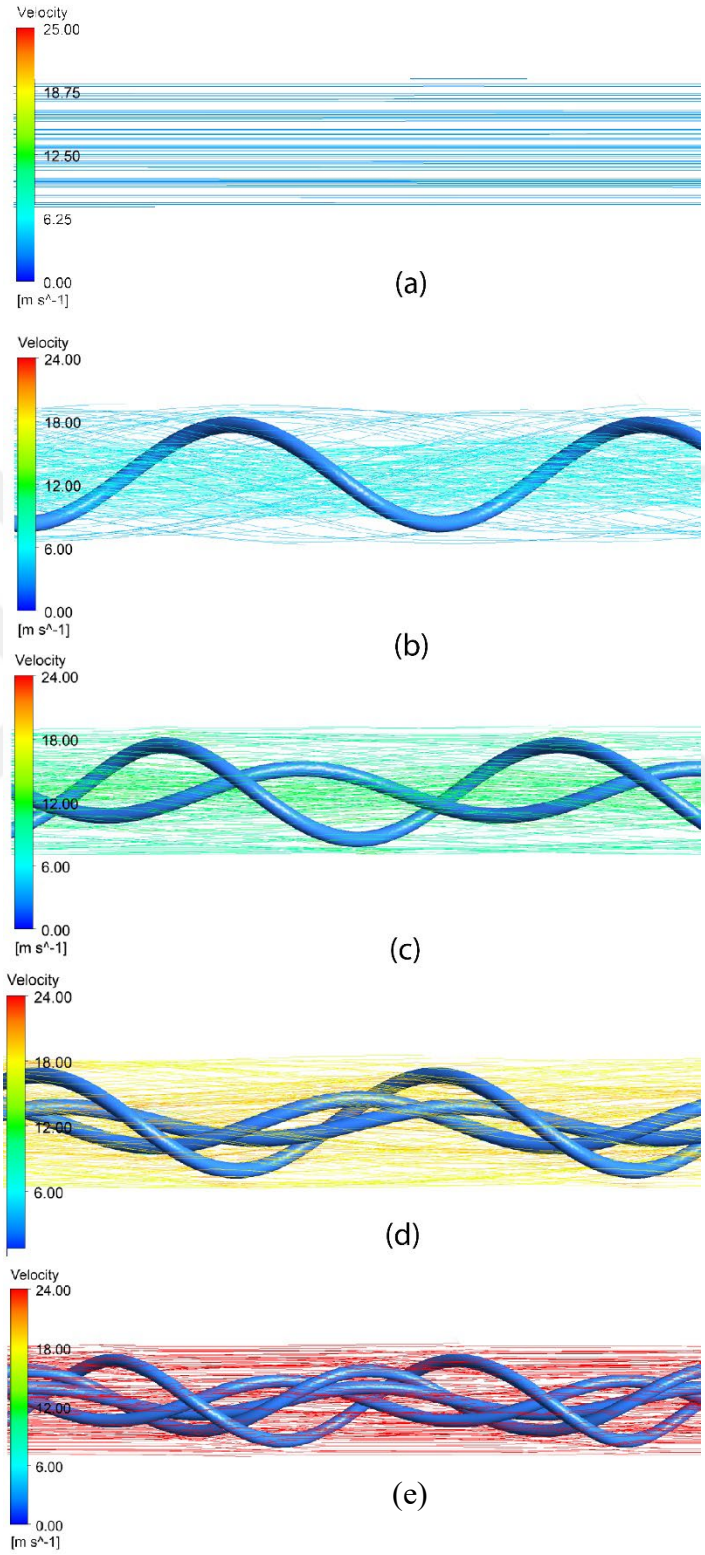

Figure 4.8 Velocity streamlines hot air inside the tube for (a) plain tube, (b) single spring, (c) double spring, (d) three springs, and (e) four springs

Figure 4.9 shows the radial velocity at Z-axis equals to (L/2) for each type and pain tube. It is indicated that the air in the smooth tube can't achieve any radial velocity where the radial velocity equals zero at Figure14.a and the radial velocity increase with the rise of the number of the springs in the tube. The velocity enhanced near to the springs so that the heat transfer increased as a result of turbulence occurred in the tube where the air get contact with the springs and change the directions. The negative velocity indicated that the direction of the flow has the opposite direction for radial direction (U direction) in these regions.

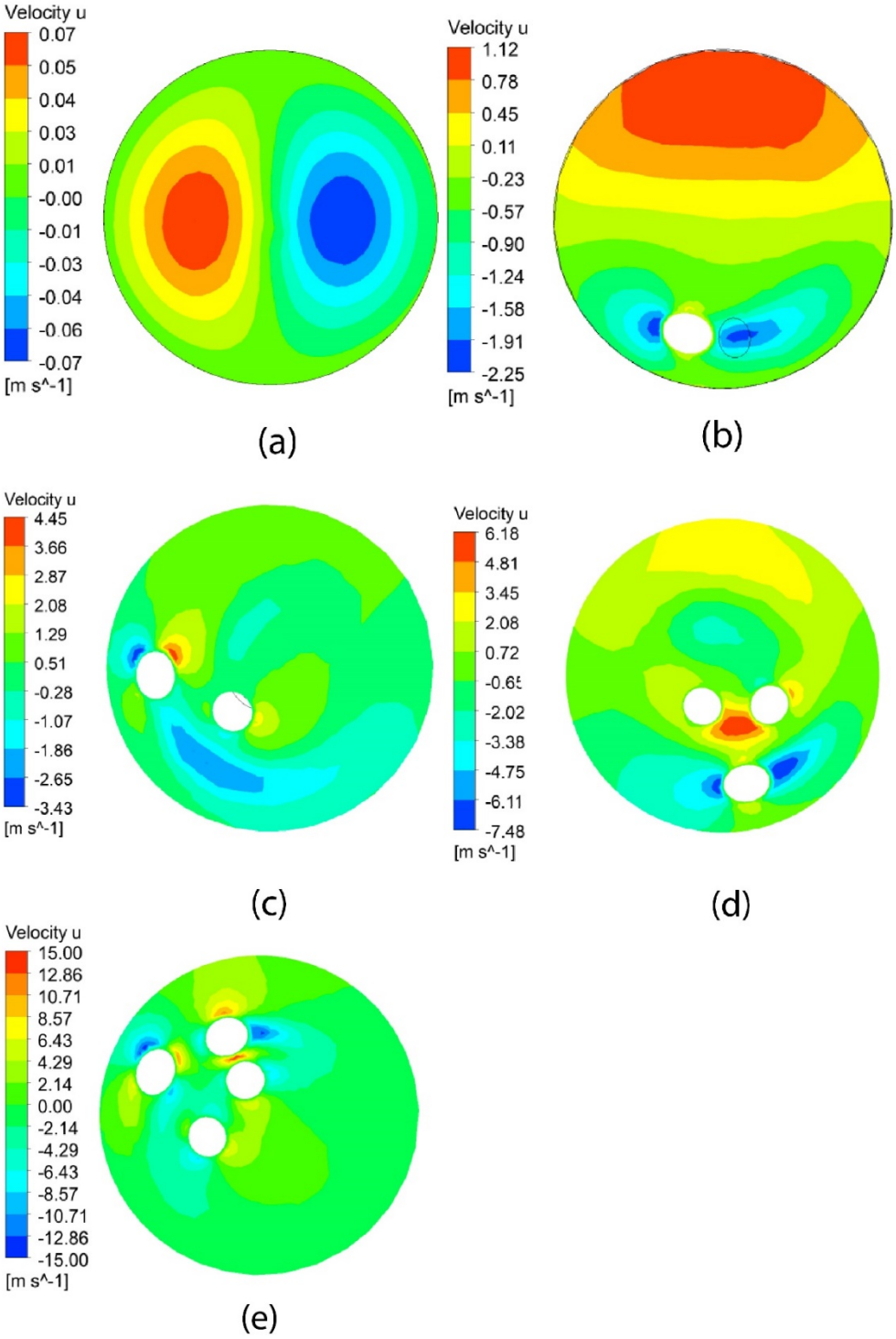

Figure 4.9 Radial velocity streamlines hot air inside the tube for (a) plain tube, (b) single spring, (c) double spring, (d) three springs and (e) four springs

4.2.7 Pressure Distribution

It is expected that the pressure increase with the turbulence motivations in the tube as seen in Figure 4.10 where the axial pressure distribution cross-plane tube. It is indicated from the figure that the total pressure has the maximum values at the inlet zone. It is seen from the setup that the boundary condition at the inlet of the tube is the mass flow rate that determines the pressure according to the geometry of the tube. The pressure at the outlet is chosen to be at zero pressure to specify the pressure drop across the tube. It is shown that the four springs achieved the highest pressure losses because of the friction between the air and the walls of the springs. The outlet pressure was set at the atmospheric pressure so that the pressure drop in the tube can be determined.

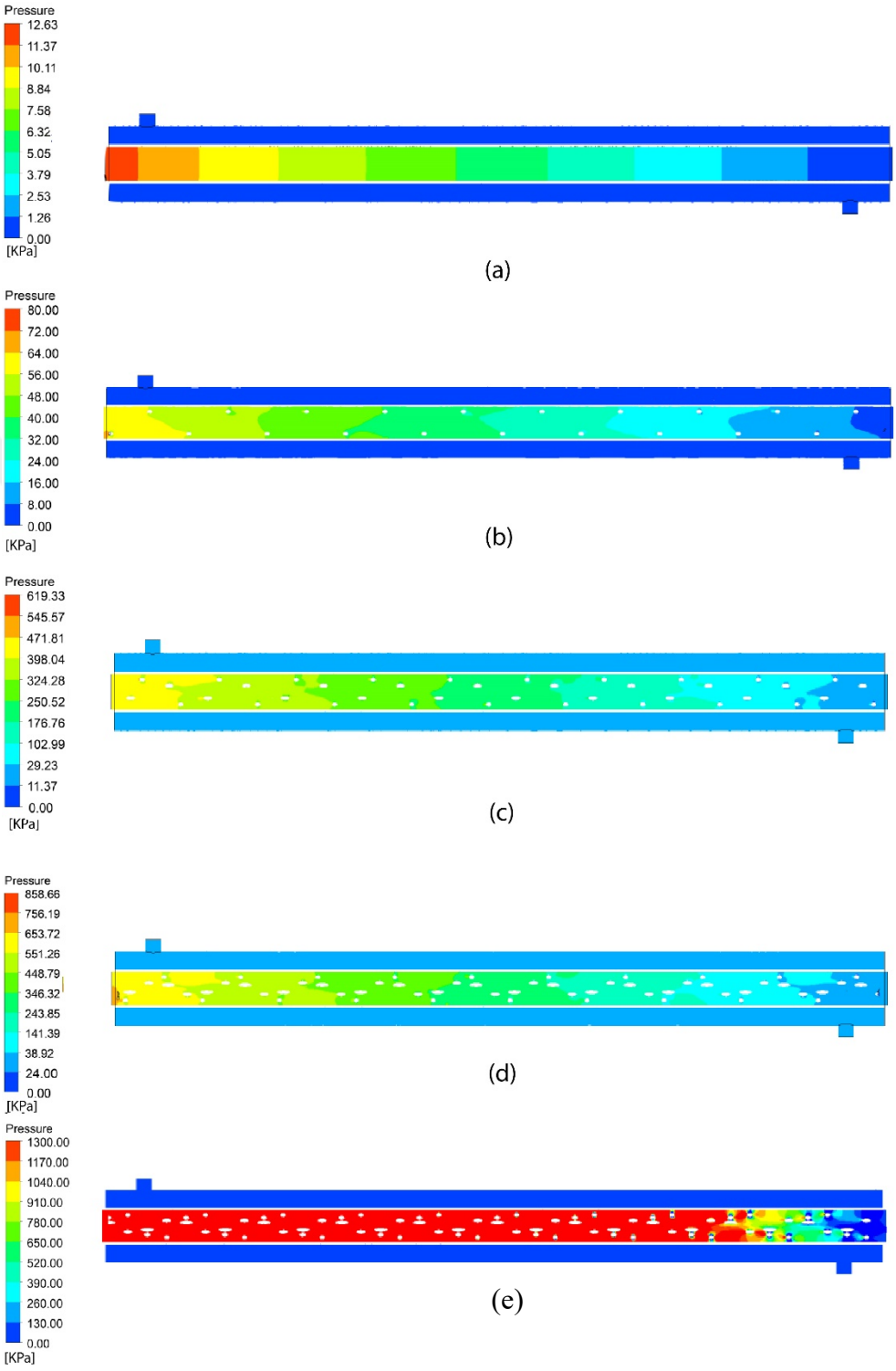

Figure 4.10: Pressure distribution in axial direction hot air inside the tube for (a) plain tube, (b) single spring, (c) double spring, (d) three springs, and (e) four springs

4.3 WIRE DIAMETER EFFECTS ON PERFORMANCE PARAMETERS

From the previous section, it is indicated that the three springs have the most influence on the cooling of air where the four springs increase the heat transfer smoothly, where, at the same time increase the pressure drop greatly. it can be concluded that the three springs utilizing for cooling air in the tube is the optimum case so that the simulation for study the effects of the wire diameter will be performed on the case of three springs.

4.3.1 Wire Diameter Effects on Nusselt number

The wire diameter of the spring utilized in this study has a great effect on the heat transfer and friction factor parameters. Figure 4.11 shows the effects of the variation of wire diameter on the Nusselt number. Three configurations of wire diameter (eg. 1mm, 2mm, and 3 mm) were used to determine the optimum wire thickness. It can be observed that the Nusselt number enhanced with the increase of Reynolds number as well as the rise of wire diameter where the wire with 3 mm achieved the maximum enhancement in heat transfer.

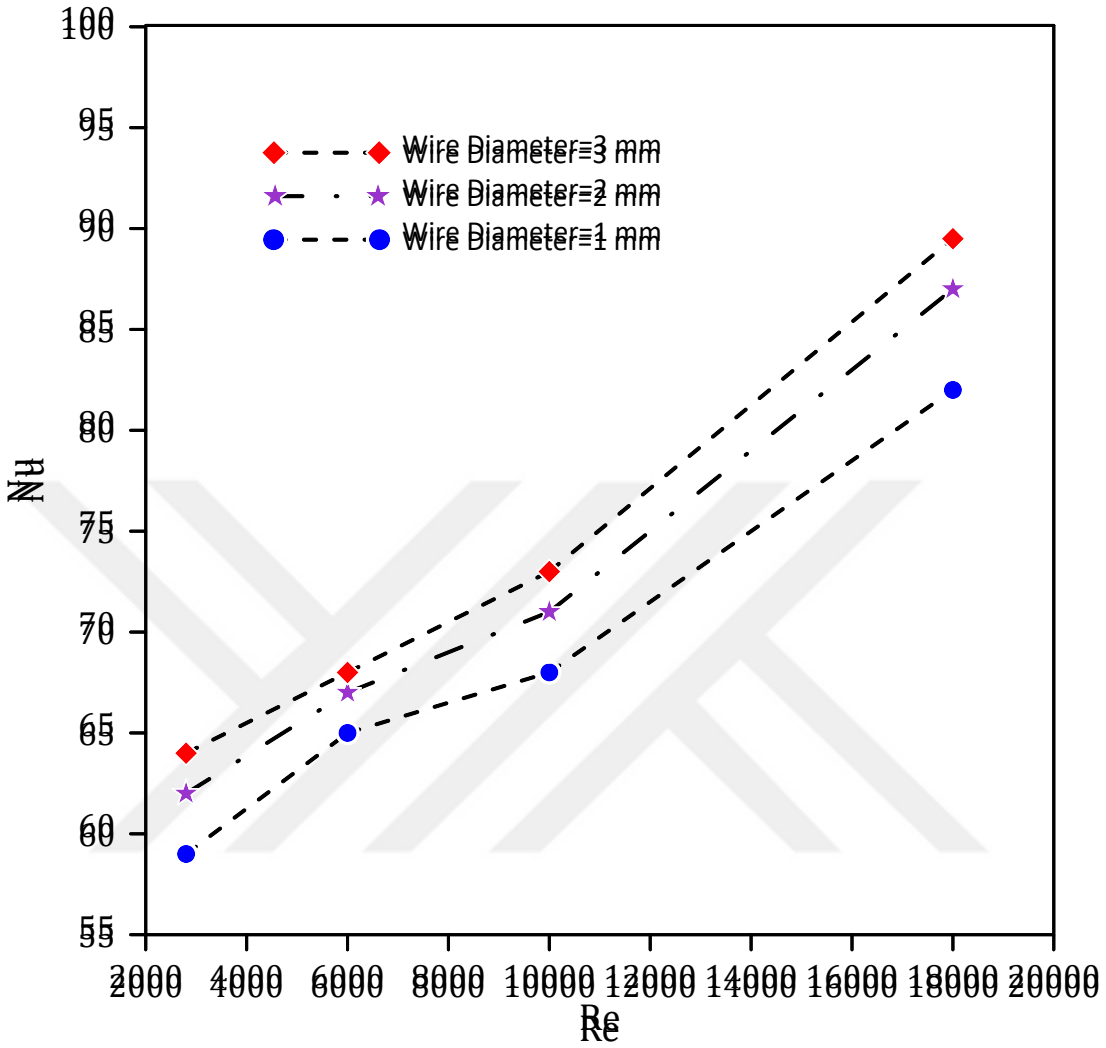

Figure 4.11 The relation between Nusselt number and Reynolds number for wire diameter configurations

4.3.2 Wire Diameter Effects on Friction Factor

Figure 4.12 displays the effects of variation of wire diameter with configurations of wire diameter 1mm, 2mm, and 3 mm on friction factor. it is indicated that the friction factor decrease with the increase of the Reynolds number and the spring wire with a 3 mm diameter achieved the maximum friction factor as the diameter increase the allowable cross-section for air passes decrease so that the pressure drop increased for this case. The three springs with a 3 mm diameter have a range of friction factor from 0.1 to 0.2 where the 1 mm diameter achieved range from 0.05 to 0.15. It can be concluded that the wire with 3 mm achieved the optimum situation.

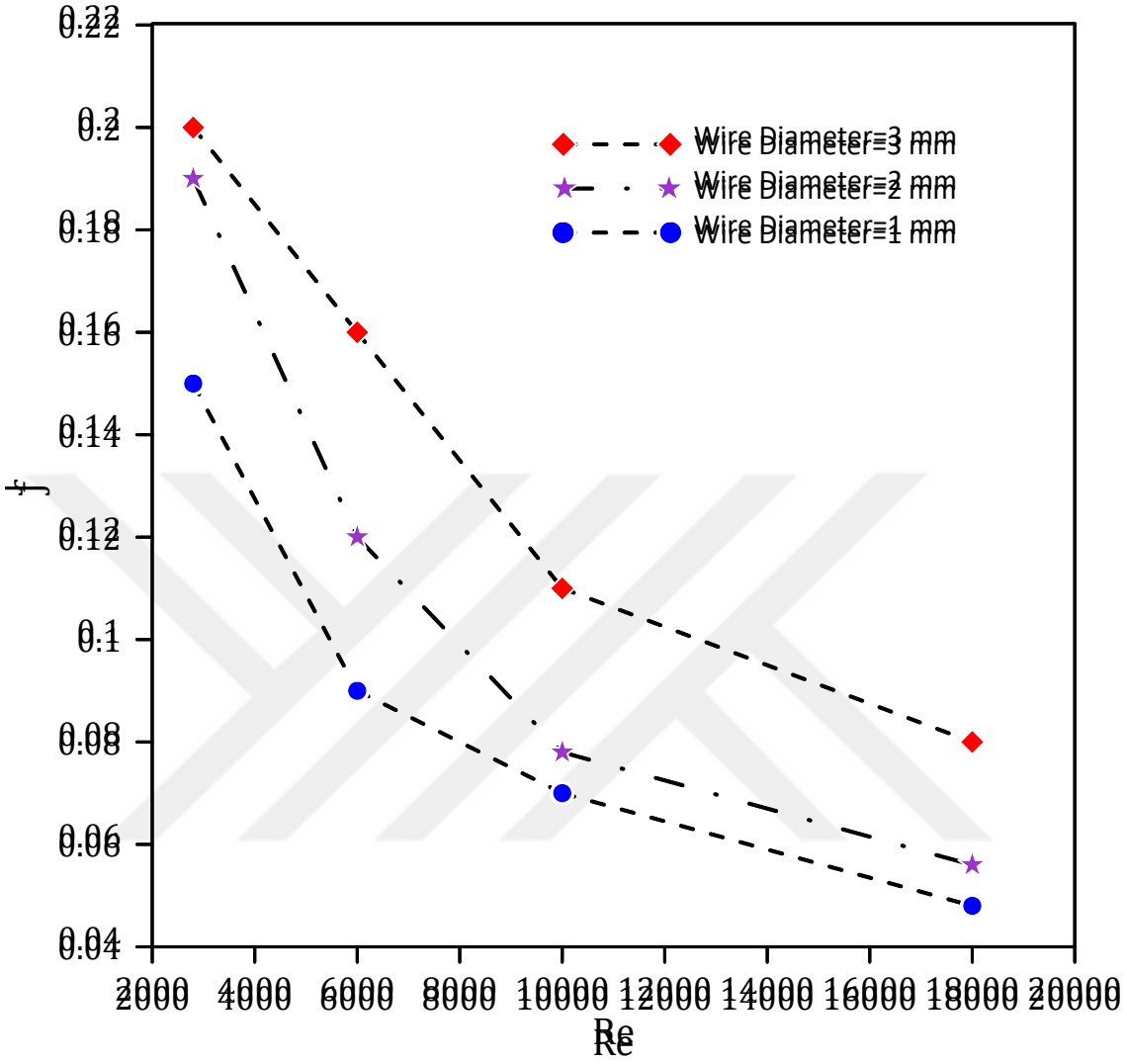

Figure 4.12 The relation between friction factor and Reynolds number for wire diameter configurations

4.3.3 Wire Diameter Effects on Exergy Efficiency

The exergy efficiency increased gradually with the rise of the Reynolds number as seen in Figure 4.13. The wire of the spring with a 3 mm diameter achieved the maximum enhancement in exergy efficiency following the figure of 48. The increase of diameter from 2 mm to 3 mm leads to an increase of the exergy efficiency with 109%.

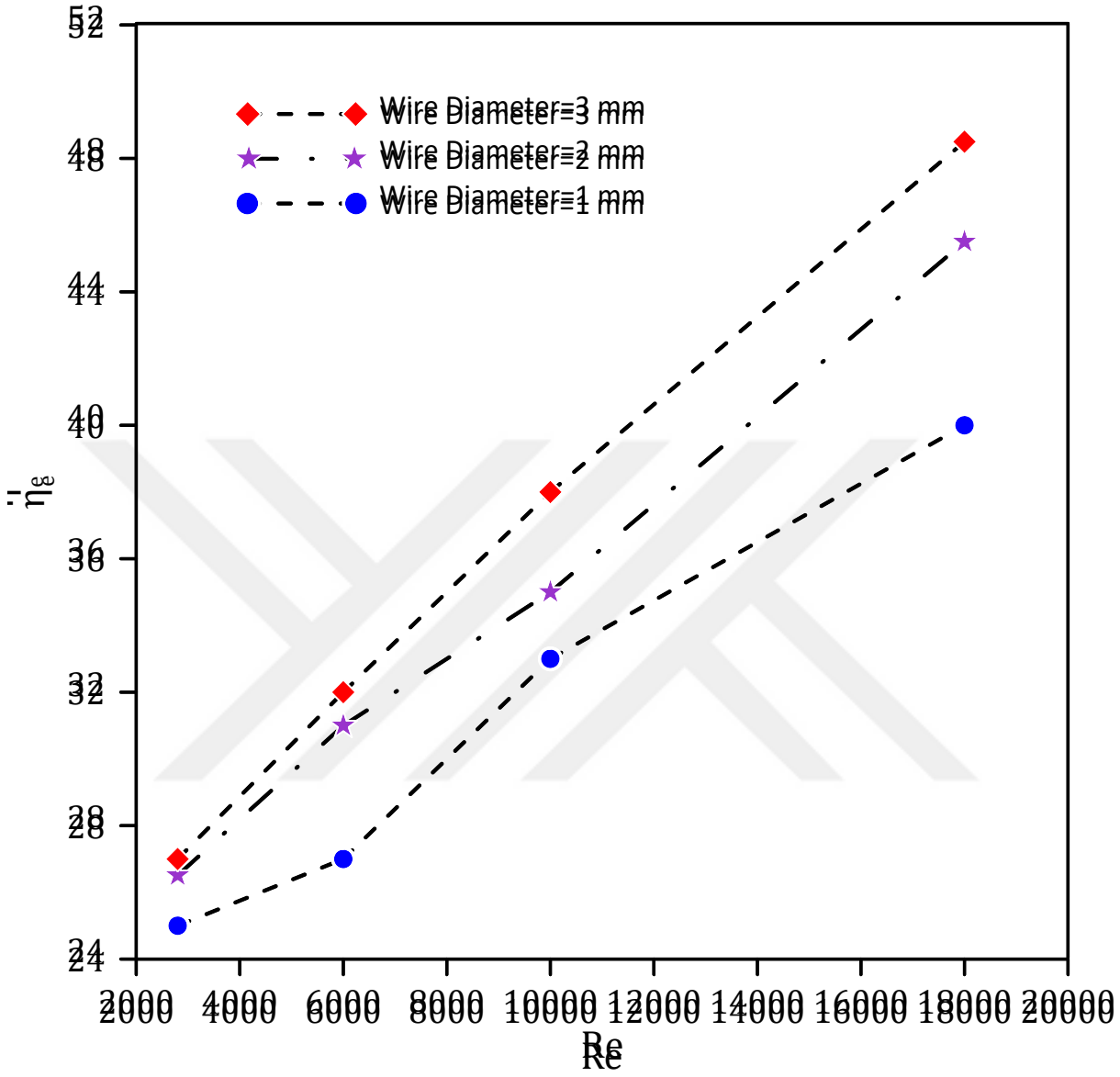

Figure 4.13 The relation between friction factor and Reynolds number for wire diameter configurations

4.3.4 Temperature and Velocity Distribution

The wire diameter affects the temperature distribution across the tube during air cooling as seen in Figure 4.14. The temperature in the middle of the tube decrease with the increase of the wire diameter and that enhances the air cooling at the end of the tube. That can be explained as the diameter of the wire increase the heat transfer during the tube increase and more heat transferred to the cold water in the anther side.

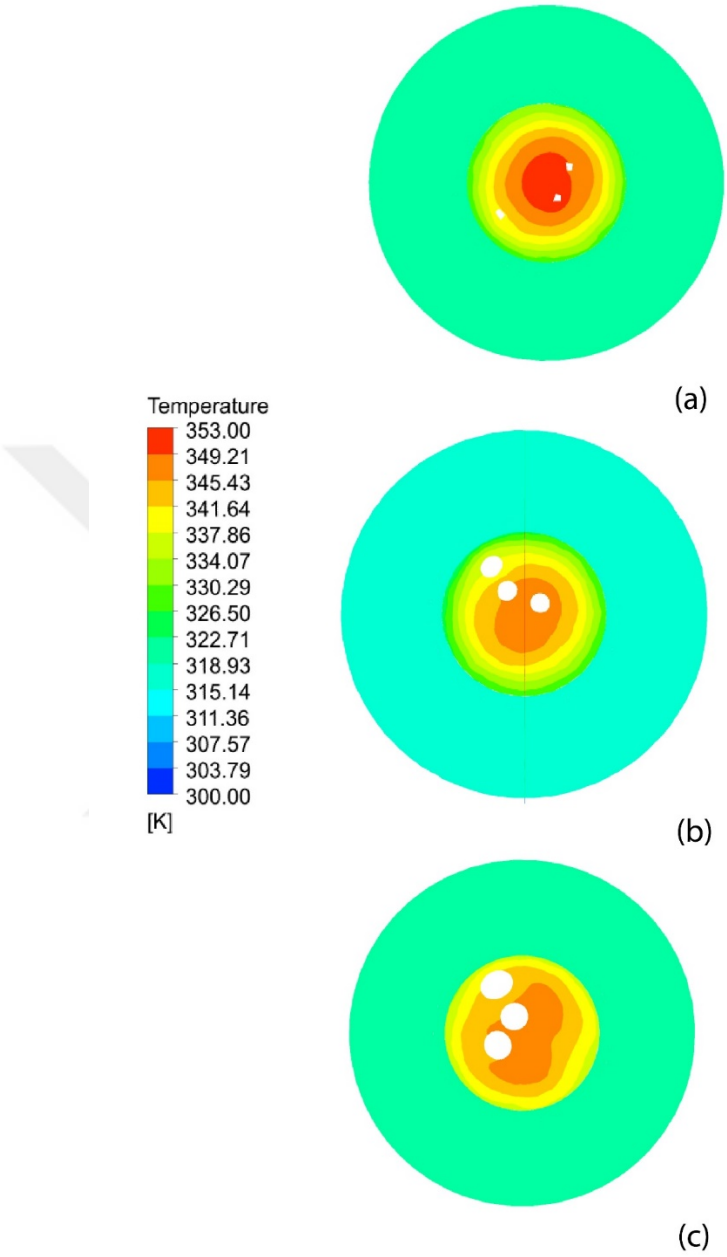

Figure 4.14 Temperature distribution at a cross-section at the middle of the tube for various wire diameters (a) t=1 mm (b) t=2 mm (c) t=3 mm

Figure 4.15 shows the vectors of velocity at cross-section for the air cooling tube for various wire diameters (1 mm, 2 mm, and 3 mm). It is indicated that the velocity increases with the rise of the wire diameter and that can be explained as the wire diameter increase the cross-section decreases so that the turbulence enhances the heat transfer from the hot air to the cold water in the anther side. Figure 4.16 displays the radial velocity of the air in the middle of the tube where there are

many changes in direction of the air vector so that the mixing between the hot and cold layers enhanced. The velocity increase leads to increase turbulence level so that the heat transfer enhanced caused air to reach less temperature.

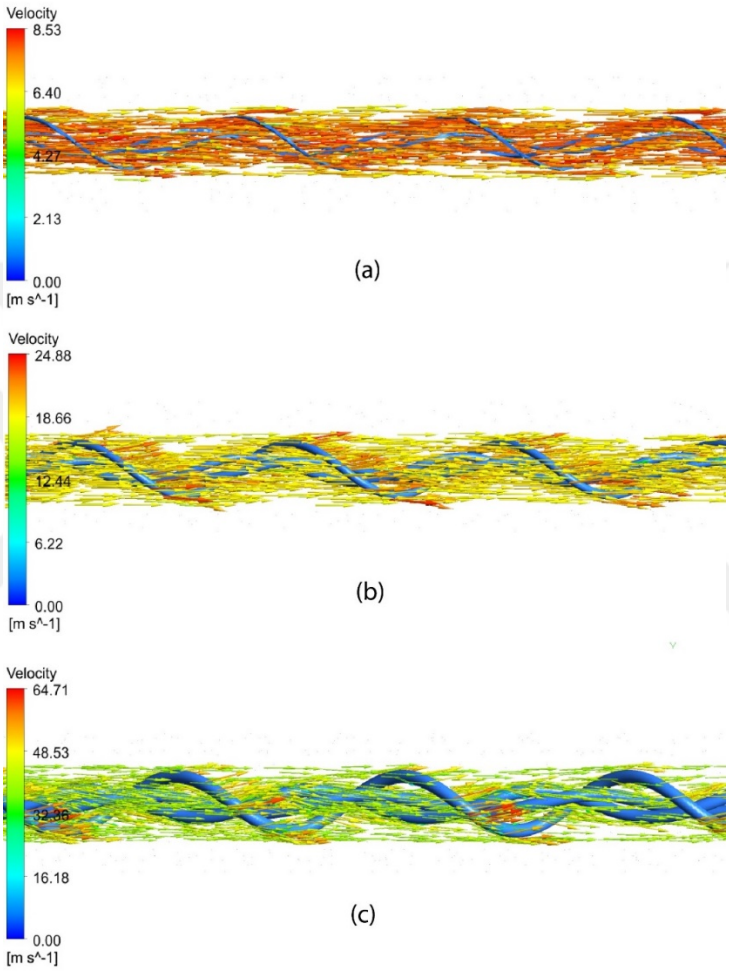

Figure 4.15 Velocity distribution at the cross-section of the tube for various wire diameters (a) t=1 mm, (b) t=2 mm, and(c) t=3 mm

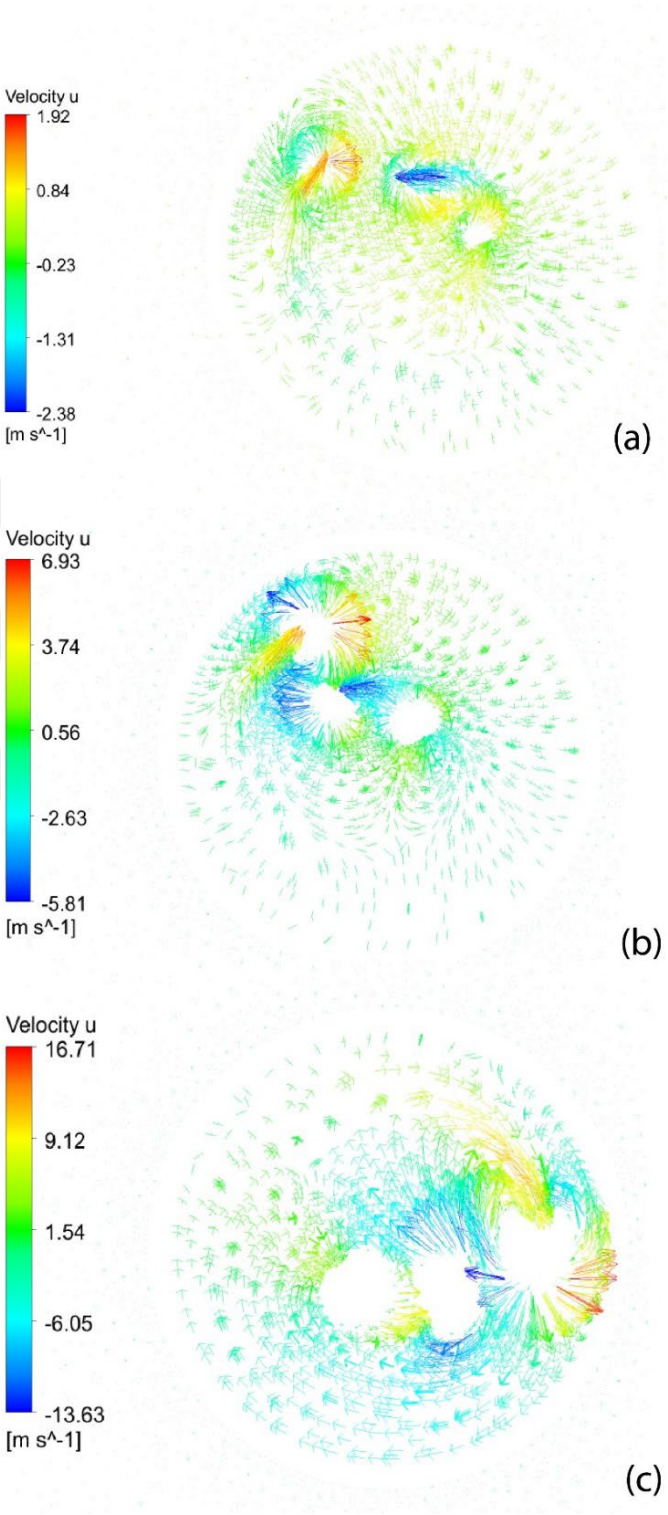

Figure 4.16 Radial velocity distribution at a cross-section at the middle of the tube for various wire diameters (a) t=1 mm, (b) t=2 mm, and(c) t=3 mm

4.4 SPRING PITCH LENGTH EFFECTS ON PERFORMANCE PARAMETERS

From the previous sections, it is indicated that the three springs with a 3mm wire diameter case have the most influence on the cooling of air performance parameters. It can be concluded that this case is the optimum case so that the simulation for study the effects of the pitch length will be performed on the case of three springs and 3 mm in diameter.

4.4.1 Pitch Length Effects on Nusselt Number

The spring pitch length applied in this study has an excessive influence on the heat transfer, friction factor, and exergy efficiency parameters. Figure 4.17 illustrates the effects of variation of pitch length on the Nusselt number. Three configurations of pitch length (eg. 10 mm, 30 mm, 50 mm, and 70 mm) were used for determining the optimum spring pitch length. It can be observed that the Nusselt number enhanced with the increase of Reynolds number as well as the rise of pitch length where the 30 mm pitch length case reached the extreme enhancement in heat transfer. The period that consumed across the length of the tube as well as the cross-section of the tube influence the Nusselt number as the more the air goes through the tube the more heat transfer. So that with the increase the Reynolds number the heat transfer crease because of the small-time and cross-section.

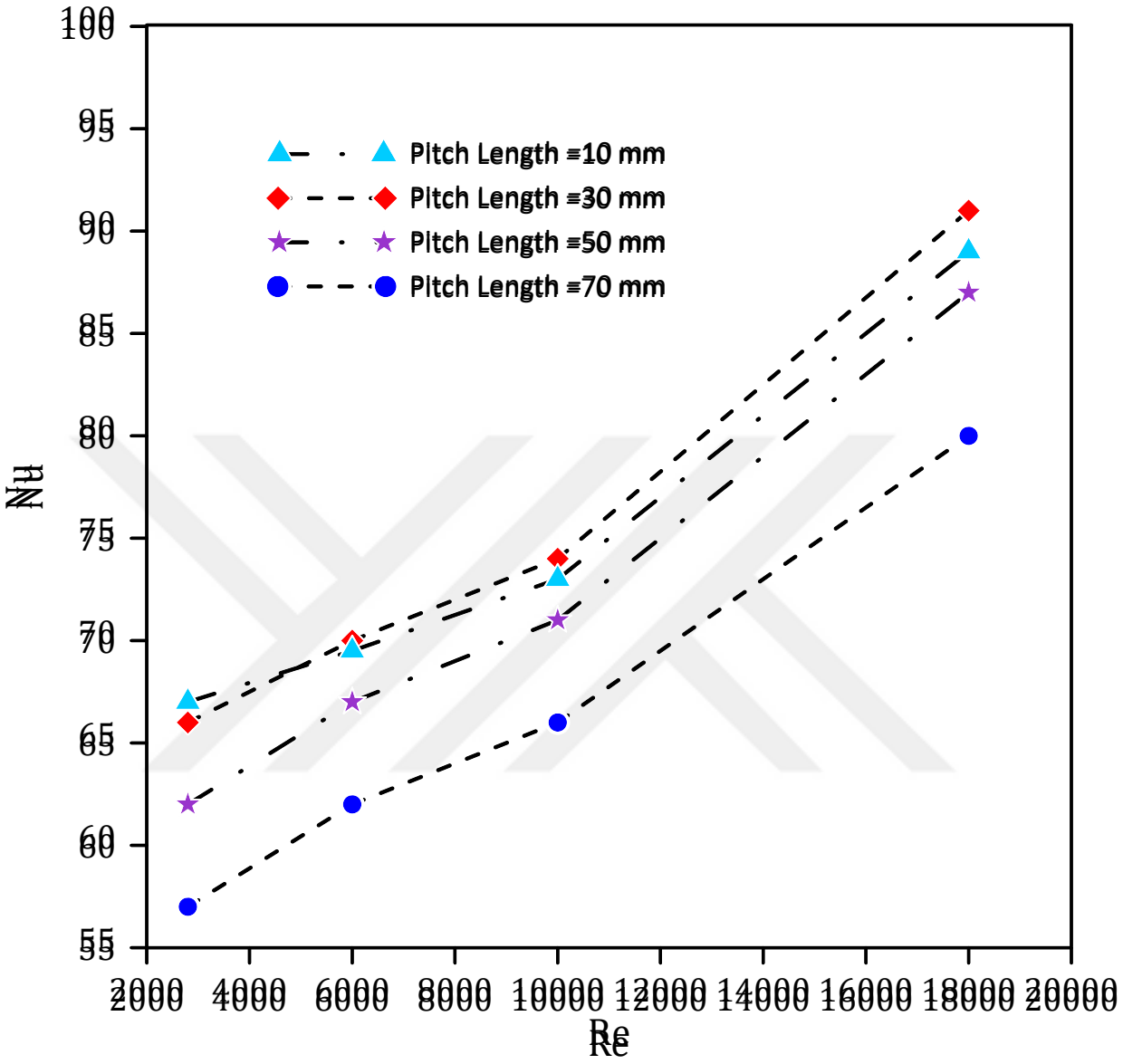

Figure 4.17 The relation between Nusselt number and Reynolds number for pitch length configurations

4.4.2 Pitch Length Effects on Friction Factor

Figure 4.18 shows the effects of variation of pitch length with configurations of spring pitch length 10mm, 30mm, 50mm, and 70 mm on friction factor. It is indicated that the friction factor decrease with the increase of the Reynolds number and the spring pitch length with 30 mm attained the maximum friction factor. The four springs with a 30 mm pitch length have a range of friction factor from 0.12 to 0.22. It is observed that the effect of the increase of friction factor resulted from

utilizing the 10 mm is more than the enhancement in heat transfer so that it is preferred to use spring with 30 mm pitch length. The impact of pressure drop increase overcome the enhancement in Nusselt number in case of 10 mm so that the author chooses the second configuration with 30 mm as an optimum choice.

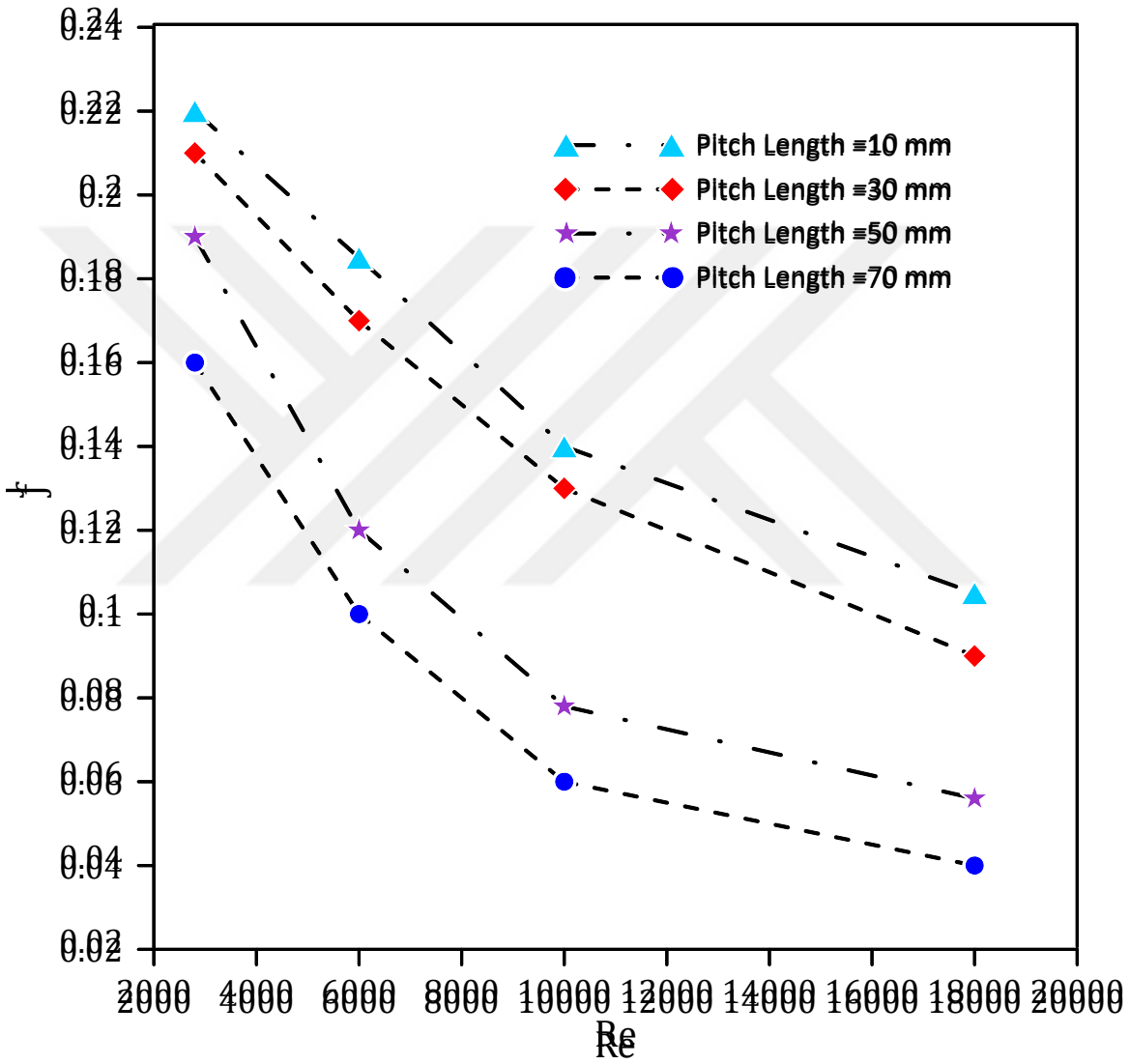

Figure 4.18 The relation between friction factor and Reynolds number for pitch length configurations

4.4.3 Pitch Length Effects on Exergy Efficiency

Figure 4.19 shows that the pitch length of the spring with 30 mm achieved the maximum enhancement in exergy efficiency following the figure of 52.

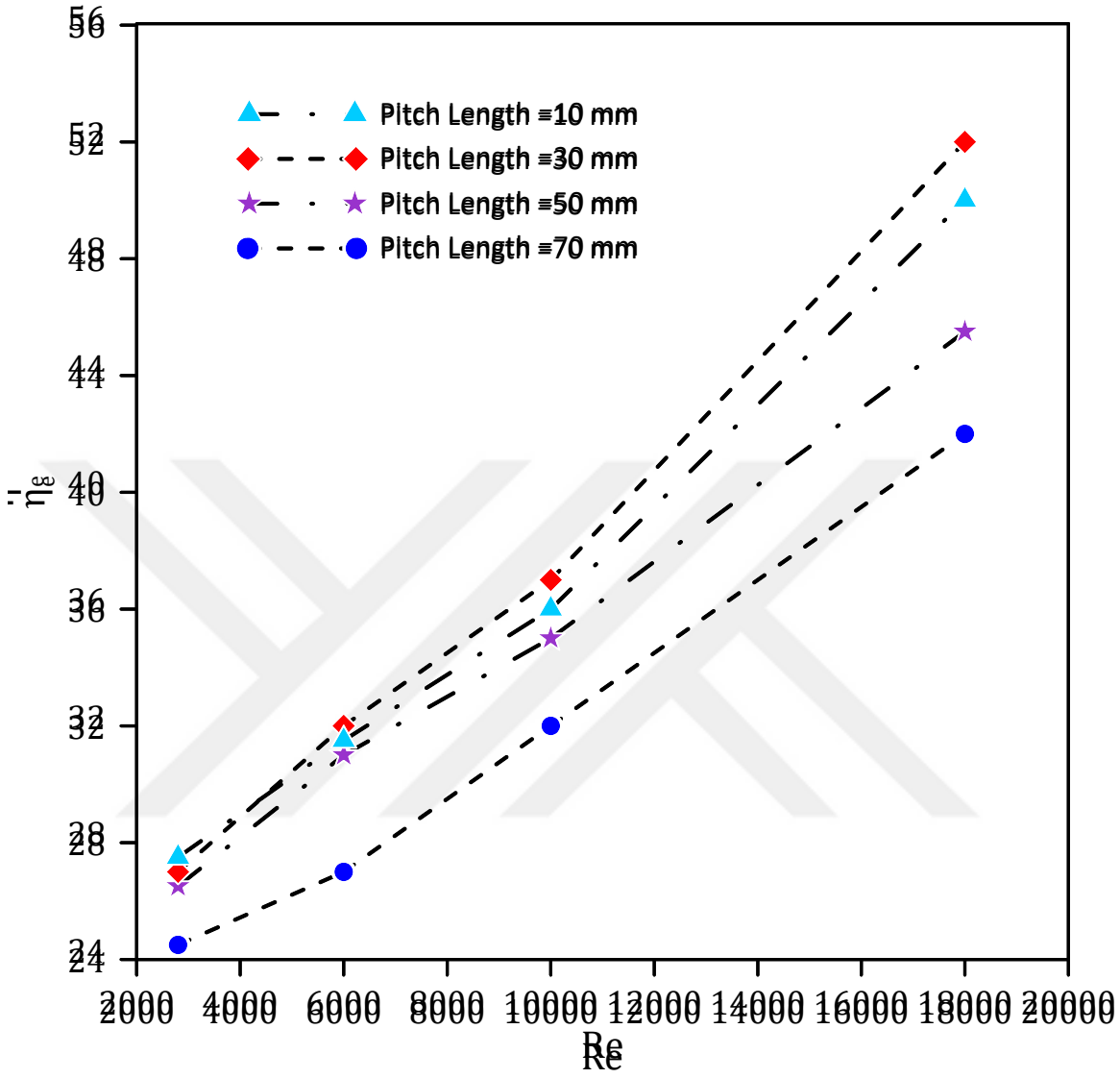

Figure 4.19 The relation between exergy efficiency and Reynolds number for pitch length configurations

4.5 THE EFFECTS OF MASS FLOW RATES CHANGES ON PERFORMANCE PARAMETERS

4.5.1 Water Volumetric Flow Rates Effects on Nusselt Number

The cold water volumetric flow rates affect the heat transfer and exergy efficiency parameters. Figure 4.20 explains the effects of variation of water volumetric flow on the Nusselt number. Three numbers of cold water volumetric flow rates (eg. 1 LPM, 2 LPM, and 3 LPM) were used to determine the optimal cold water volumetric flow rate. It can be observed that the Nusselt number

enhanced with the increase of Reynolds number as well as the rise of cold water volumetric flow rates.

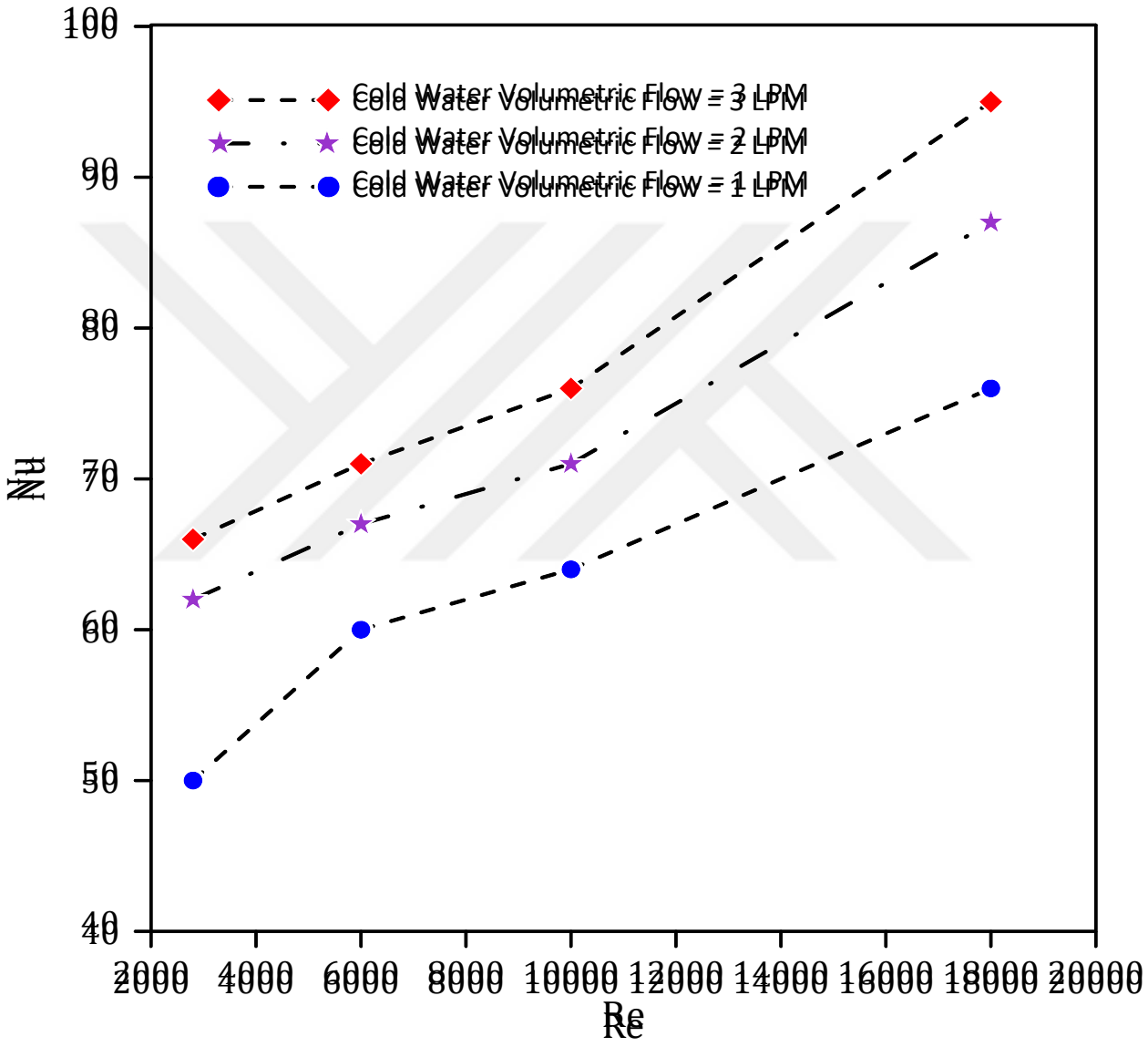

Figure 4.20 The relation between Nusselt number and Reynolds number for volumetric flow rate configurations

4.5.1 Water Volumetric Flow Rates Effects on Exergy Efficiency

It is indicated that the exergy efficiency increased gradually with the rise of the Reynolds number as seen in Figure 4.21. The cold water volumetric flow rates at 3 LPM achieved the maximum enhancement in exergy efficiency following the figure of 52.

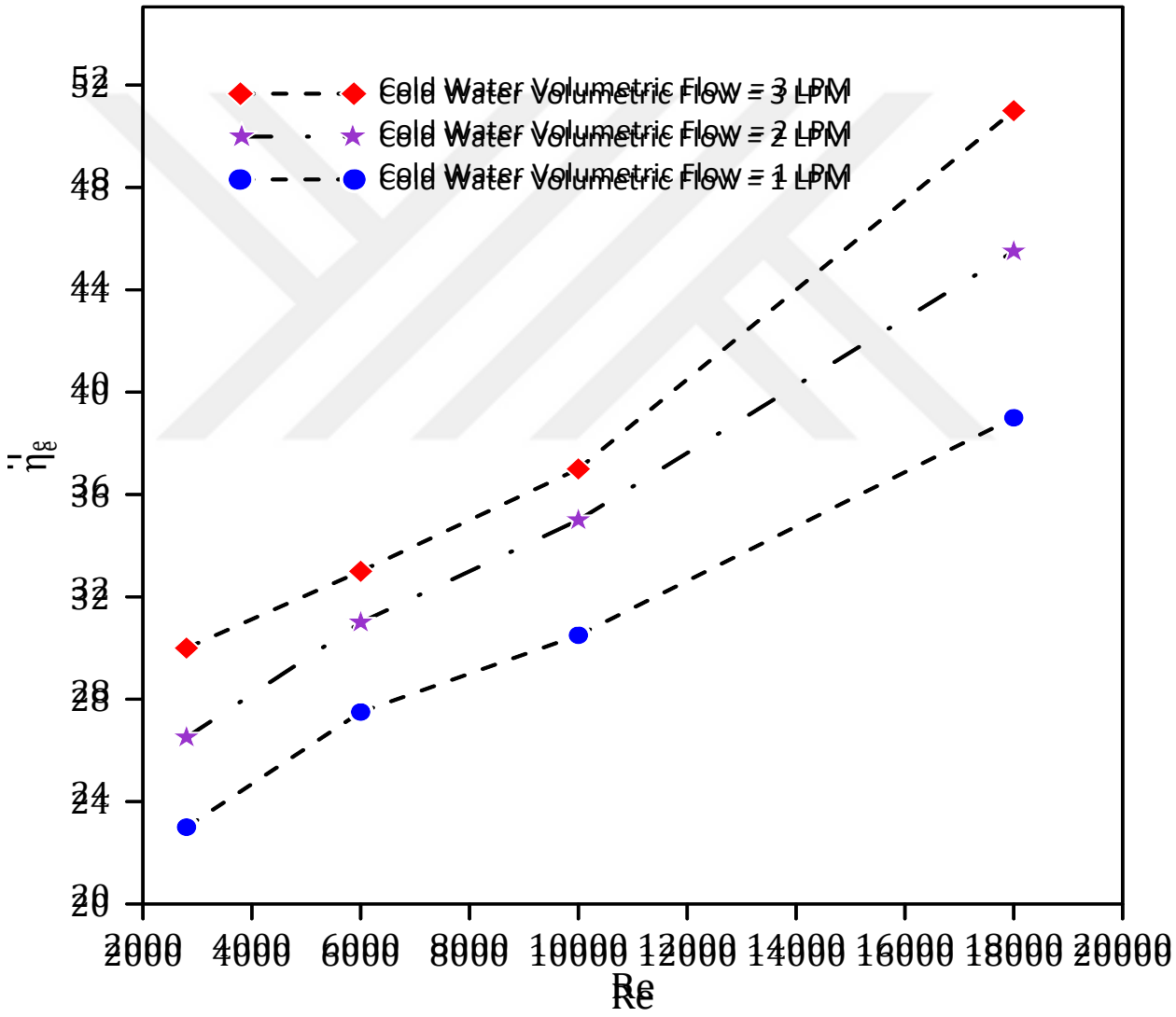

Figure 4.21 The relation between exergy efficiency and Reynolds number for volumetric flow rate configurations

5 CONCLUSION

In this paper, a numerical study of the effect of multi-spring wire on heat transfer, friction factor and exergy losses introduced to increase cooling of air in tubes as the application of air conditioning the results can be concluded that follow:

- The thermal parameters such as Nusselt Number and heat flux and hydraulic performance like friction factor and exergy efficiency will be studied for a range of Reynolds number from 2800 to 18000. It can be concluded that the wire spring leads to an increase in the Nusslet number so that the heat transfer coefficients and heat flux increased.
- The four spring achieved the highest value of enhancement of air cooling comparing to five, tribe, and single, double springs, and plain tubes. The four spring's configuration has the highest heat flux following the figure of 322 to 399 W/m^2. Heat transfer increases easily through the flow and swirls cause flow to be turbulent which led to even better convection heat transfer.
- Friction factor decrease with the rise of the Reynolds number and the five spring has the maximum pressure drop comparing to other configurations. The exergy efficiency is the highest with the four spring configuration.
- It can be observed that the Nusselt number enhanced with the increase of wire diameter where the wire with 3 mm achieved the maximum enhancement in heat transfer. The four springs with a 3 mm diameter have a range of friction factor from 0.1 to 0.2 where the 1 mm diameter achieved range from 0.05 to 0.15. It can be concluded that the wire with 3 mm achieved the optimum situation. The increase of diameter from 2 mm to 3 mm leads to an increase of the exergy efficiency with 109%.
- It can be detected that the Nusselt number improved with the rise of pitch length where the 30 mm pitch length case reached the extreme enhancement in heat transfer. The impact of pressure drop increase overcome the enhancement in Nusselt number in case of 30 mm so that the other choose the second configuration with 50 mm as an optimum choice.
- Three numbers of cold water volumetric flow rates (eg. 1 LPM, 2 LPM, and 3 LPM) were used to determine the optimal cold water volumetric flow rate. It can be observed that the

Nusselt number enhanced with the increase of Reynolds number as well as the rise of cold water volumetric flow rates.

- The optimum condition has four springs with a 3 mm wire diameter and 30 mm pitch length where the volumetric flow rate that achieved the optimization was 3 LPM.

REFERENCES

[1] N. Chaiyat, Energy and economic analysis of a building air-conditioner with a phase change material (PCM), Energy Conversion and Management, 94 (2015) 150-158.

[2] S. Al-Fahed, W. Chakroun, Effect of tube-tape clearance on heat transfer for fully developed turbulent flow in a horizontal isothermal tube, International Journal of Heat and Fluid Flow, 17 (1996) 173-178.

[3] Y.T. Kang, R. Stout, R.N. Christensen, The effects of inclination angle on flooding in a helically fluted tube with a twisted insert, International Journal of Multiphase Flow, 23 (1997) 1111-1129.

[4] M. Takahashi, Y. Momozaki, Pressure drop and heat transfer of a mercury single-phase flow and an air–mercury two-phase flow in a helical tube under a strong magnetic field, Fusion Engineering and Design, 51-52 (2000) 869-877.

[5] S.K. Saha, A. Dutta, S.K. Dhal, Friction and heat transfer characteristics of laminar swirl flow through a circular tube fitted with regularly spaced twisted-tape elements, International Journal of Heat and Mass Transfer, 44 (2001) 4211-4223.

[6] H.Y. Kim, S. Koyama, W. Matsumoto, Flow pattern and flow characteristics for counter-current two-phase flow in a vertical round tube with wire-coil inserts, International Journal of Multiphase Flow, 27 (2001) 2063-2081.

[7] C. Aprea, C. Renno, Experimental analysis of a transfer function for an air cooled evaporator, Applied Thermal Engineering, 21 (2001) 481-493.

[8] L. Wang, B. Sundén, Performance comparison of some tube inserts, International Communications in Heat and Mass Transfer, 29 (2002) 45-56.

[9] S.-S. Hsieh, F.-Y. Wu, H.-H. Tsai, Turbulent heat transfer and flow characteristics in a horizontal circular tube with strip-type inserts. Part I. Fluid mechanics, International Journal of Heat and Mass Transfer, 46 (2003) 823-835.

[10] W.H. Azmi, K.V. Sharma, P.K. Sarma, R. Mamat, S. Anuar, L. Syam Sundar, Numerical validation of experimental heat transfer coefficient with SiO2 nanofluid flowing in a tube with twisted tape inserts, Applied Thermal Engineering, 73 (2014) 296-306.

[11] V. Özceyhan, Conjugate heat transfer and thermal stress analysis of wire coil inserted tubes that are heated externally with uniform heat flux, Energy Conversion and Management, 46 (2005) 1543-1559.

[12] A. Tandiroglu, Effect of flow geometry parameters on transient heat transfer for turbulent flow in a circular tube with baffle inserts, International Journal of Heat and Mass Transfer, 49 (2006) 1559-1567.

[13] P. Naphon, Heat transfer and pressure drop in the horizontal double pipes with and without twisted tape insert, International Communications in Heat and Mass Transfer, 33 (2006) 166-175.

[14] Y.-W. Chiu, J.-Y. Jang, 3D numerical and experimental analysis for thermal–hydraulic characteristics of air flow inside a circular tube with different tube inserts, Applied Thermal Engineering, 29 (2009) 250-258.

[15] S.W. Chang, A.W. Lees, H.-T. Chang, Influence of spiky twisted tape insert on thermal fluid performances of tubular air–water bubbly flow, International Journal of Thermal Sciences, 48 (2009) 2341-2354.

[16] D.A. Yadav, Effect of Half Length Twisted-Tape Turbulators on Heat Transfer and Pressure Drop Characteristics inside a Double Pipe U-Bend Heat Exchanger, (2009).

[17] C. Thianpong, P. Eiamsa-ard, K. Wongcharee, S. Eiamsa-ard, Compound heat transfer enhancement of a dimpled tube with a twisted tape swirl generator, International Communications in Heat and Mass Transfer, 36 (2009) 698-704.

[18] S. Eiamsa-ard, K. Wongcharee, P. Eiamsa-ard, C. Thianpong, Heat transfer enhancement in a tube using delta-winglet twisted tape inserts, Applied Thermal Engineering, 30 (2010) 310-318.

[19] J. Guo, A. Fan, X. Zhang, W. Liu, A numerical study on heat transfer and friction factor characteristics of laminar flow in a circular tube fitted with center-cleared twisted tape, International Journal of Thermal Sciences, 50 (2011) 1263-1270.

[20] B. Salam, S. Biswas, S. Saha, M.M.K. Bhuiya, Heat Transfer Enhancement in a Tube using Rectangular-cut Twisted Tape Insert, Procedia Engineering, 56 (2013) 96-103.

[21] S.D. Salman, A.A.H. Kadhum, M.S. Takriff, A.B. Mohamad, CFD Analysis of Heat Transfer and Friction Factor Characteristics in a Circular Tube Fitted with Quadrant-Cut Twisted Tape Inserts, Mathematical Problems in Engineering, 2013 (2013) 1-8.

[22] A. Hasanpour, M. Farhadi, K. Sedighi, A review study on twisted tape inserts on turbulent flow heat exchangers: The overall enhancement ratio criteria, International Communications in Heat and Mass Transfer, 55 (2014) 53-62.

[23] V. Mokkapati, C.-S. Lin, Numerical study of an exhaust heat recovery system using corrugated tube heat exchanger with twisted tape inserts, International Communications in Heat and Mass Transfer, 57 (2014) 53-64.

[24] C. Vashistha, A.K. Patil, M. Kumar, Experimental investigation of heat transfer and pressure drop in a circular tube with multiple inserts, Applied Thermal Engineering, 96 (2016) 117-129.

[25] A. Kumar, S. Chamoli, M. Kumar, Experimental investigation on thermal performance and fluid flow characteristics in heat exchanger tube with solid hollow circular disk inserts, Applied Thermal Engineering, 100 (2016) 227-236.

[26] A.R. Singh Suri, A. Kumar, R. Maithani, Effect of square wings in multiple square perforated twisted tapes on fluid flow and heat transfer of heat exchanger tube, Case Studies in Thermal Engineering, 10 (2017) 28-43.

[27] A. Gomaa, M.A. Halim, A.M. Elsaid, Enhancement of cooling characteristics and optimization of a triple concentric-tube heat exchanger with inserted ribs, International Journal of Thermal Sciences, 120 (2017) 106-120.

[28] Y. Sun, Z. Guan, K. Hooman, A review on the performance evaluation of natural draft dry cooling towers and possible improvements via inlet air spray cooling, Renewable and Sustainable Energy Reviews, 79 (2017) 618-637.

[29] M.R. Esfahani, E.M. Languri, Exergy analysis of a shell-and-tube heat exchanger using graphene oxide nanofluids, Experimental Thermal and Fluid Science, 83 (2017) 100-106.

[30] M.A. Omara, M.A. Abdelatief, Experimental study of heat transfer and friction factor inside elliptic tube fixed with helical coils, Applied Thermal Engineering, 134 (2018) 407-418.

[31] A.T. Wijayanta, I. Yaningsih, M. Aziz, T. Miyazaki, S. Koyama, Double-sided delta-wing tape inserts to enhance convective heat transfer and fluid flow characteristics of a double-pipe heat exchanger, Applied Thermal Engineering, 145 (2018) 27-37.

[32] A. Bazgir, N. Nabhani, S. Eiamsa-ard, Numerical analysis of flow and thermal patterns in a double-pipe Ranque-Hilsch vortex tube: Influence of cooling a hot-tube, Applied Thermal Engineering, 144 (2018) 181-208.

[33] Y. Yang, G. Cui, C.Q. Lan, Developments in evaporative cooling and enhanced evaporative cooling - A review, Renewable and Sustainable Energy Reviews, 113 (2019) 109230.

[34] M. Jeong, M.Y. Ha, Y.G. Park, Numerical investigation of heat transfer enhancement in a dimpled cooling channel with different angles of the vortex generator, International Journal of Heat and Mass Transfer, 144 (2019).

[35] S. Khorasani, S. Jafarmadar, S. Pourhedayat, M.A.A. Abdollahi, A. Heydarpour, Experimental investigations on the effect of geometrical properties of helical wire turbulators on thermal performance of a helically coiled tube, Applied Thermal Engineering, 147 (2019) 983-990.

[36] H. Qin, C. Wang, M. Wang, D. Zhang, W. Tian, G.H. Su, S. Qiu, Numerical investigation on thermal-hydraulic characteristics of NaK in a helical wire wrapped annulus, International Journal of Heat and Mass Transfer, 145 (2019).

[37] M.A. Sayed, A.M.T.A. Eldein Hussin, W. Aboelsoud, N.A. Mahmoud, Performance evaluation of Wire Mesh Heat Exchangers, Applied Thermal Engineering, (2019).

[38] L. Zhang, X. Song, X. Zhang, Theoretical analysis of exergy destruction and exergy flow in direct contact process between humid air and water/liquid desiccant solution, Energy, 187 (2019) 115976.

[39] X. Zhang, B. Liu, J. Liu, X. Wang, H. Zhang, Experimental and numerical analysis of heat transfer and flow characteristics in parabolic ducts, International Journal of Heat and Mass Transfer, 147 (2020).

[40] M.E. Nakhchi, J.A. Esfahani, K.C. Kim, Numerical study of turbulent flow inside heat exchangers using perforated louvered strip inserts, International Journal of Heat and Mass Transfer, 148 (2020).

[41] A.R. Rahmati, A. Gheibi, Experimental and numerical analysis of a modified hot water radiator with improved performance, International Journal of Thermal Sciences, 149 (2020).

[42] A. Jafarzad, M.M. Heyhat, Thermal and exergy analysis of air- nanofluid bubbly flow in a double-pipe heat exchanger, Powder Technology, (2020).

[43] D.C. Planchard, SOLIDWORKS 2018 Tutorial with Video Instruction, Better Textbooks, (2018).

[44] S.A. Marzouk, M.M. Abou Al-Sood, E.M.S. El-Said, M.K. El-Fakharany, Effect of wired nails circular–rod inserts on tube side performance of shell and tube heat exchanger: Experimental study, Applied Thermal Engineering, 167 (2020) 114696.

[45] M. Sugawara, M. Tago, Freezing of water in a closed vertical tube cooled by air flow, International Journal of Heat and Mass Transfer, 133 (2019) 800-811.

[46] D. Boelter, The Dittus-Boelter Equation, (2002).